SCIENCE CHINA
Information Sciences

• RESEARCH PAPER •

May 2026, Vol. 69, Iss. 5, 152206:1–152206:19
https://doi.org/10.1007/s11432-025-4782-0

Dynamic-event-based distributed cooperative learning of unknown nonlinear systems over directed connected graphs

Shi-Lu DAI*, Penghai WEN & Min WANG

School of Automation Science and Engineering, South China University of Technology, Guangzhou 510641, China

Received 8 March 2025/Revised 16 September 2025/Accepted 3 January 2026/Published online 24 March 2026

Abstract Distributed cooperative learning (DCL) provides an efficient modeling/identification approach for unknown dynamics of multi-agent systems by exploiting the learning capacity of neural networks (NNs) in a collaborative fashion. However, all existing DCL frameworks require the communication topology among agents to be undirected. This paper proposes a DCL algorithm featuring a dynamic event-triggered mechanism over directed connected graphs for a group of uncertain nonlinear systems. The Laplacian matrices of directed graphs do not possess the positive semi-definite property, which significantly complicates the extension of DCL from undirected graphs to directed graphs. First, NN identifiers with cooperative NN weight updating laws are constructed within the context of dynamic event-triggered communication. Second, after ensuring finite-time convergence of the state estimate error subsystems, a novel group-convergence-proof strategy is presented for the identification error systems, and then it is rigorously proved that the NN weight estimates of all agents converge to a small neighborhood of their common optimal values. Third, the unknown nonlinear dynamics are accurately identified along the union of system trajectories of all agents. Compared with static event triggering, the proposed dynamic event-triggered mechanism extends the triggering thresholds while maintaining learning performance, thereby further reducing the communication burden. Finally, the advantages and effectiveness of the proposed DCL algorithm are demonstrated through a simulation example.

Keywords distributed cooperative learning, directed connected graphs, dynamic event-triggered communication, multi-agent systems, system identification

Citation Dai S-L, Wen P H, Wang M. Dynamic-event-based distributed cooperative learning of unknown nonlinear systems over directed connected graphs. Sci China Inf Sci, 2026, 69(5): 152206, https://doi.org/10.1007/s11432-025-4782-0

1 Introduction

Identification of complex systems has attracted widespread attention due to its critical importance across numerous scientific and engineering domains, including fault diagnosis [1, 2], image processing [3], and model-based control [4–7]. Neural networks (NNs) have emerged as powerful and effective tools for the online intelligent identification of nonlinear dynamic systems, primarily due to their universal approximation capabilities [8]. A substantial body of research has demonstrated successful outcomes in NN-based identification and control [9–15]. Through Lyapunov stability analysis, these approaches provide theoretical guarantees for small estimation errors in system states. However, the convergence of NN weight estimates to their ideal or optimal values is rarely addressed, which limits the full exploitation of the NN learning capabilities. Consequently, when faced with similar or identical nonlinear systems, online retraining of NNs is still inevitable due to the absence of knowledge acquisition from prior identification tasks.

Learning can be conceptualized as a process of acquiring and accumulating knowledge. The persistent excitation (PE) condition plays a pivotal role in enabling effective learning for NNs. Nevertheless, verifying the satisfaction of the PE condition a priori is highly challenging. To address this challenge, a dynamic learning (DL) framework was introduced in [16] for second-order Brunovsky systems. In this framework, it was rigorously demonstrated that the local basis function subvector of a radial basis function (RBF) NN, evaluated along a recurrent input trajectory, satisfies a partial PE condition. This enabled a rigorous convergence analysis of NN weight estimates, leading to an accurate approximation of unknown system dynamics. Building upon this foundation, the DL framework was extended to high-order nonlinear systems in normal form using the state transformation technique [17, 18]. Furthermore, by integrating backstepping design with dynamic surface control, the DL approach was generalized to

* Corresponding author (email: audaisl@scut.edu.cn)

high-order strict-feedback systems [19]. Under the DL framework, numerous studies on adaptive NN identification and learning control have been reported, including [20–27].

It is important to note that the experiential knowledge acquired through the aforementioned DL approaches is typically confined to the vicinity of a single recurrent trajectory. In contrast to single-agent learning, cooperative learning in multi-agent systems offers distinct advantages, such as broader generalization domains, improved fault tolerance, and enhanced robustness. Inspired by consensus theory [28], a distributed cooperative identification method was proposed in [29] under undirected topologies, leveraging convergence results for a class of linear time-varying systems with cooperative PE conditions. By integrating DL with a distributed cooperative strategy [29], distributed cooperative DL algorithms were developed for multi-agent homogeneous systems in [30–32]. These approaches introduced cooperative learning terms into NN weight update laws, enabling agents to share weight estimates with neighbors via network communication. As a result, each agent can learn the experiential knowledge along the union trajectory of all agents, thereby enhancing the learning generalization capability of NNs. Considering practical constraints, cooperative DL with prescribed performance has been applied to multiple autonomous vehicles [33–36]. To reduce the communication burden and save network bandwidth between adjacent agents, a static event-triggered communication mechanism with a time-dependent exponentially decaying threshold was incorporated into the cooperative DL framework [37, 38]. However, these methods are restricted to undirected communication topologies.

In many practical engineering applications, such as the World Wide Web and mobile broadcast networks [39], certain agents may only possess signal transmitters or receivers, resulting in unidirectional information flow [40]. Compared to undirected topologies, directed topologies offer distinct advantages, including broader applicability, improved robustness, enhanced fault tolerance, and reduced communication resource consumption [41]. Hence, developing a cooperative DL algorithm under directed topologies is of considerable theoretical and practical significance. Moreover, distributed cooperative learning (DCL) involves the transmission of high-dimensional NN weight estimates, which can consume substantial network resources. Particularly during the early learning phase, when agents have not yet completed their individual learning tasks, inaccurate weight estimates may be transmitted, potentially degrading the learning performance of neighboring agents. Event-triggered communication mitigates this issue by initiating transmissions only when local updates exceed a predefined threshold, thereby significantly reducing communication overhead. This mechanism optimizes bandwidth allocation, alleviates synchronization constraints, and ensures convergence, making it particularly suitable for resource-constrained networked control systems such as the Internet of Things (IoT), multi-agent collaborative systems, and embedded systems. However, existing event-triggering schemes in cooperative DL algorithms rely on static triggering conditions, where the thresholds remain fixed and cannot be adaptively adjusted based on the current system states. Compared to static event-triggering [42], dynamic event-triggering mechanisms offer a more efficient means of reducing triggering frequency and conserving network resources [43–45]. Hence, establishing cooperative DL results under dynamic event-triggered communication remains an important research challenge.

This paper addresses the DCL problem for a class of uncertain multi-agent systems over directed connected graphs. The primary challenges can be summarized as follows. First, existing Lyapunov stability analyses for the overall identification error system and convergence analyses of NN weight estimation errors across all agents heavily rely on the positive semi-definiteness of Laplacian matrices. For example, the exponential stability theorem for a class of linear time-varying (LTV) systems presented in [29] serves as the foundation for verifying uniform convergence of NN weight estimates among all agents. This result assumes that the Laplacian matrices are positive semi-definite, which is essential for achieving cooperative DL. However, from a mathematical perspective, the Laplacian matrices of directed connected graphs generally lack symmetry and, consequently, do not possess the positive semi-definite property. This poses a significant challenge for the stability analysis of the identification error system and the convergence verification of NN weight estimates. Second, the dynamic event-triggered threshold varies with the current NN weight estimates of each agent, introducing additional complexity in ensuring both learning accuracy and system stability. Therefore, designing a dynamic event-triggering mechanism that guarantees learning performance is another significant concern.

Considering the specific characteristics of Laplacian matrices associated with directed graphs, this paper proposes a novel group-convergence-proof strategy for analyzing the stability of state estimate error subsystems and the convergence of NN weight estimate error subsystems. First, a parametric Lyapunov function independent of Laplacian matrices is employed. Second, by estimate applying M-matrix theory [46], all adaptive identification system signals are proven to remain bounded, and the state estimate error subsystems are shown to converge to a small neighborhood of the origin within finite time. Third, it is observed that a directed connected graph can be regarded as the union of directed trees in which each node serves as the root node. This insight leads to a novel perspective: each agent learns the unknown system dynamics based on its own experienced trajectory and then

shares the learned knowledge with the connected agents via the directed tree in which it serves as the root node. In this manner, all agents achieve cooperative learning through knowledge exchange among connected agents. Inspired by this idea, a group-convergence-proof strategy is introduced for the NN weight estimate error systems, where the NN weight estimates of each agent are grouped into N sets based on N experienced trajectories from N agents. A novel Lyapunov function is constructed by combining the converse Lyapunov lemma with the directed trees lemma, and then the NN weight estimates in each group are shown to converge to a small neighborhood of their ideal values. Thus, the convergence analysis of weight estimates is completed without relying on the positive semi-definiteness of Laplacian matrices. Finally, internal dynamic variables are introduced to design the dynamic triggering thresholds. All internal dynamic variables are proven to remain positive and converge to a small neighborhood around the origin, the size of which can be specified by design. Theoretical analysis demonstrates that these internal dynamic variables effectively enlarge the event-triggered thresholds, thereby further reducing the number of triggering events compared to static event triggering. Moreover, the convergence of internal dynamic variables ensures learning accuracy with less data being transferred. Additionally, the Zeno phenomenon is successfully avoided. For clarity, the innovations and contributions are summarized as follows.

(1) Unlike the cooperative DL approaches presented in [29–32, 34–38], which are established over undirected communication topology, the proposed DCL algorithm is developed over directed connected graphs. Accurate NN identification of unknown system dynamics is successfully achieved along the union of the system trajectories of all agents. Notably, the cooperative system identification method remains effective even when bidirectional information exchange is not feasible due to communication constraints. Since undirected graphs are a special case of directed graphs, the proposed cooperative DL algorithm demonstrates enhanced robustness and broader applicability compared to undirected graph-based approaches.

(2) Compared with the existing cooperative DL results [30–32, 34–38], which depend heavily on the positive semi-definiteness of Laplacian matrices corresponding to communication graphs, this paper proposes an M-matrix-based parameterized Lyapunov function to perform stability analysis. The cooperative learning terms in the NN weight updating laws are treated as interactive perturbations. Furthermore, a graph decomposition approach is introduced to reformulate the multi-agent distributed cooperative learning problem into two components: a virtual leader's independent learning subtask and a virtual follower's consensus tracking problem. A group-convergence-proof strategy, in which each agent acts as a virtual leader, is developed to rigorously establish the consensus convergence of NN weight estimates to their common ideal values.

(3) In contrast to static event-triggered communication [37,38], this paper introduces internal dynamic variables to design a dynamic event-triggered condition. The event-triggered thresholds vary dynamically based on the weight information of each agent, effectively reducing the number of event triggers compared to static event-triggered communication while ensuring approximation performance. The self-adaptive regulation mechanism inherent in the dynamic event-triggered communication significantly improves communication bandwidth and energy efficiency in networked distributed systems performing cooperative DL, particularly in scenarios involving high-dimensional NN weight interactions.

Notation. $\mathbb{R}$, $\mathbb{R}^{\geqslant 0}$, $\mathbb{R}^m$, and $\mathbb{R}^{m\times n}$ denote, respectively, the set of real numbers, non-negative real numbers, m-dimensional real vectors, and real matrices with m rows and n columns. $\mathbb{N}$ is the set of natural numbers. I_n is the n-dimensional identity matrix, and I is an identity matrix with the appropriate dimension. $\lambda_{\max}(A)$ and $\lambda_{\min}(A)$ represent the maximum and minimum eigenvalues of matrix A, respectively. $(\cdot)^\top$ signifies the transpose of a matrix or vector.

2 Problem formulation and preliminaries

2.1 Problem formulation

Consider a multi-agent system consisting of N agents (vertices), under a directed topology $\mathcal{G} = \{\mathcal{V}, \mathcal{E}\}$, where $\mathcal{V} = \{\upsilon_1, \upsilon_2, \ldots, \upsilon_N\}$ denotes the vertex set, and $\mathcal{E} \subseteq \mathcal{V}\times\mathcal{V}$ is the directed edge set which shows the communication connection between different agents. The system dynamics of the i-th agent with $i \in \mathcal{N} = \{1, 2, \ldots, N\}$ is given by

$$\dot{x}_i = H\left(x_i, u_i(t)\right), \tag{1}$$

where $u_i(t) \in \mathbb{R}^m$ and $x_i = [x_{i1}, x_{i2}, \ldots, x_{in}]^\top \in \mathbb{R}^n$ denote the system input and state vector, respectively; $H\left(x_i, u_i(t)\right) = \left[h_1\left(x_i, u_i(t)\right), h_2\left(x_i, u_i(t)\right), \ldots, h_n\left(x_i, u_i(t)\right)\right]^\top$ is the unknown smooth nonlinear functions. Let $\xi_i(t) = [x_i(t)^\top, u_i(t)^\top]^\top \in \mathbb{R}^{n+m}$. Thus, the identified system (1) can be rewritten as

$$\dot{x}_i = H\left(\xi_i(t)\right). \tag{2}$$

The following assumption is commonly made in the dynamic learning literature, e.g., [1,30,31,34–38].

Assumption 1. The identified system (1) is supposed to be stable, which means that the trajectory $\varphi(\xi_i(t))$, $i \in \mathcal{N}$, generated by (1), remains in a bounded compact set $\Omega_{\xi i}$, i.e., $\varphi(\xi_i(t)) \in \Omega_{\xi i} \subset \mathbb{R}^{n+m}$, $\forall t \geqslant t_0$, with $t_0 \geqslant 0$ being the initial moment. Moreover, each system trajectory $\varphi(\xi_i(t))$, $i \in \mathcal{N}$ is in a recurrent motion.

The identification objective is to propose an NN-based DCL algorithm for a multi-agent system (1) over a directed connected graph to achieve the locally accurate NN identification of unknown system dynamics $H(\cdot)$.

2.2 Algebraic graph theory

The information interaction between N agents is modeled as a directed graph $\mathcal{G} = (\mathcal{V}, \mathcal{E})$. For two distinct nodes $\upsilon_1, \upsilon_2 \in \mathcal{V}$, only when node υ_2 can receive the messages coming from node υ_1, we have $(\upsilon_1, \upsilon_2) \in \mathcal{E}$. Assume $A = [a_{ij}]_{N\times N}$ signifies the weighted adjacency matrix corresponding to $\mathcal{G}$, where $a_{ij} > 0$ only when $(\upsilon_j, \upsilon_i) \in \mathcal{E}$, and otherwise $a_{ij} = 0$. All nodes are supposed to possess no self edges, i.e., $a_{ii} = 0$, $i \in \mathcal{N}$. If there exists a sequence of edges $\{(\upsilon_1, \varpi_1), (\varpi_1, \varpi_2), \ldots, (\varpi_{k-1}, \varpi_k), (\varpi_k, \upsilon_2)\} \subset \mathcal{E}$, then node υ_1 possesses a path towards node υ_2. If there exists at least a path, for any two different nodes of $\mathcal{G}$, then $\mathcal{G}$ is a strongly connected graph. Assume node υ_i, $i \in \mathcal{N}$ owns paths towards all other nodes υ_j, $j \in \mathcal{N}$, $j \neq i$, and then $\mathcal{G}$ is called to cover a directed spanning tree with υ_i being the root node. Further, if $\mathcal{G}$ covers only one directed spanning tree and there are no edges towards the root node, then $\mathcal{G}$ is referred to as a directed tree. $L = [l_{ij}]_{N\times N}$ means the Laplacian matrix of graph $\mathcal{G}$, where $l_{ij} = -a_{ij}$ when $i \neq j$, and $l_{ii} = \sum_{j=1}^{N} a_{ij}$. In the field of leader-following consensus, after defining an additional leader node υ_0, graph $\mathcal{G}$ can be expanded to the augmented graph $\bar{\mathcal{G}} = (\bar{\mathcal{V}}, \bar{\mathcal{E}})$, with $\bar{\mathcal{V}} = \{\upsilon_0, \upsilon_1, \ldots, \upsilon_N\}$ and $\bar{\mathcal{E}} = \bar{\mathcal{V}} \times \bar{\mathcal{V}}$. The leader υ_0 can only transmit information to its neighborhoods, but not receive any information from followers υ_i, $i \in \mathcal{N}$. Define the adjacency matrix between the leader and the followers as $B = \mathrm{diag}\{b_1, b_2, \ldots, b_N\}$, where $b_i > 0$, $i \in \mathcal{N}$ only when node υ_i can receive information from node υ_0. Moreover, denote the leader-following matrix of $\bar{\mathcal{G}}$ as $H = B + L$.

Assumption 2. The information interaction topology $\mathcal{G}$ between N agents is a strongly connected directed graph.

Remark 1. The requirement for a strongly connected communication topology, as stated in Assumption 2, stems from the fundamental structure of the cooperative DL framework. Within this framework, each agent is responsible for accurately identifying the unknown nonlinear function within a local region around its own stable operating trajectory, while concurrently sharing its acquired knowledge with all other agents through the network. In the absence of strong connectivity (e.g., if the topology contains only a directed spanning tree), at least one agent would be unable to propagate its learned knowledge to all other agents. This disruption in the information flow inevitably results in the failure of distributed cooperative DL, as achieving consistent global knowledge alignment becomes unattainable.

The directed trees lemma is given as follows, which will be used in the convergence verification of NN weight estimates.

Lemma 1 (Directed trees lemma [47])**.** Assume the augmented graph $\bar{\mathcal{G}}$ contains a directed spanning tree, and then the leader-following matrix H is nonsingular. Moreover, there exist positive definite matrices P_1 and Q_1 satisfying

$$q' = [q'_1, \ldots, q'_N]^\top = H^{-1}1_N, \quad P_1 = \mathrm{diag}(1/q'_i),\ Q_1 = P_1H + H^\top P_1. \tag{3}$$

2.3 RBF NNs and PE condition

2.3.1 *Universal approximation of RBF NNs*

Any unknown continuous function $h(\xi) : \mathbb{R}^q \to \mathbb{R}$ can be effectively approximated over a compact set Ω_ξ by RBF NNs [8] with enough NN nodes, that is,

$$h(\xi) = W^{*\top}\Phi(\xi) + \varepsilon(\xi), \quad \forall \xi \in \Omega_\xi, \tag{4}$$

where $W^* \in \mathbb{R}^l$ denotes the ideal/optimal NN weight vector with $l \geqslant 1$ being the number of NN nodes, $\Phi(\xi) = [\phi_1(\xi), \phi_2(\xi), \ldots, \phi_l(\xi)]^\top \in \mathbb{R}^l$ signifies the basis function vector, and $\varepsilon(\xi)$ represents the approximation error satisfying $\|\varepsilon(\xi)\| \leqslant \varepsilon^*$ with ε^* being an adequately small positive constant. Gaussian functions are selected as the basis functions in this paper, that is, $\phi_i(\xi) = \exp[-(\xi - \pi_i)^\top(\xi - \pi_i)/\kappa_i^2]$ $(i = 1, 2, \ldots, l)$, where $\pi_i = [\pi_{i1}, \pi_{i2}, \ldots, \pi_{iq}]^\top$ and κ_i denote the NN center and width, respectively.

2.3.2 *Localized approximation of RBF NNs*

For localized NNs (e.g., Gaussian RBF NNs), the output values of neural nodes distant from a fixed NN input become negligible. Consequently, the output of the NN corresponding to any recurrent input trajectory can be accurately approximated by a partial subset of nodes in close proximity to the trajectory. Any unknown continuous function can be approximated excellently over a compact region along a recurrent input $\xi(t) \in \Omega_\xi$ by partial RBF NN nodes [16] near the input trajectory $\xi(t)$, that is,

$$h(\xi) = W_\zeta^{*\top} \Phi_\zeta(\xi) + \varepsilon_\zeta(\xi), \tag{5}$$

where $W_\zeta^* \in \mathbb{R}^{l_\zeta}$ with $l_\zeta < l$, $\Phi_\zeta(\xi) = [\phi_{a_1}(\xi), \phi_{a_2}(\xi), \ldots, \phi_{a_{l_\zeta}}(\xi)]^{\mathrm{T}} \in \mathbb{R}^{l_\zeta}$, and $\varepsilon_\zeta(\xi)$ denotes the ideal weight vector, basis function vector, and corresponding approximation error of the localized NNs, respectively, and $|\|\varepsilon_\zeta(\xi)\| - \|\varepsilon(\xi)\||$ is adequately small.

2.3.3 *Persistent excitation (PE) condition*

Definition 1 (PE condition [16])**.** A time-varying matrix $\Phi(t) : \mathbb{R}^{\geqslant 0} \to \mathbb{R}^{a \times b}$ is called to be persistently exciting, if and only if $\Phi(t)$ is bounded and there exist positive constants a_0, a_1, and T satisfying

$$a_0 I \leqslant \int_{t_0}^{t_0+T} \Phi(t)\Phi^\top(t)dt \leqslant a_1 I, \quad \forall t_0 \in R^{\geqslant 0}. \tag{6}$$

Lemma 2 (PE condition satisfaction [16])**.** For any recurrent continuous trajectory $\xi(t) : [0, \infty) \to \Omega_\xi$ where Ω_ξ is a compact set, if the RBF NN $W^\top \Phi(\xi)$ with its centers localized in a regular lattice which is large enough to cover Ω_ξ, then the RBF NN subvector $\Phi_\zeta(\xi(t))$, consisting of those NN nodes which are located in a small neighborhood of the recurrent trajectory $\xi(t)$, is persistently exciting.

2.4 Useful lemmas

Here, we give some useful lemmas that will be used in the subsequent sections.

Lemma 3 ([46])**.** There exists a positive definite diagonal matrix $D \in \mathbb{R}^{a \times a}$, such that $DP_2 + P_2^\top D = Q_2$ with Q_2 being positive definite, if and only if $P_2 = [p_{ij}]_{a \times a}$ is an M-matrix. If the matrix P_2 possesses non-positive off-diagonal elements and the leading principal minors of P_2 are positive, that is,

$$\det \begin{bmatrix} p_{11} & p_{12} & \cdots & p_{1k} \\ p_{21} & p_{22} & \cdots & p_{2k} \\ \vdots & \vdots & \ddots & \vdots \\ p_{k1} & p_{k2} & \cdots & p_{kk} \end{bmatrix} > 0, \quad k = 1, 2, \ldots, a, \tag{7}$$

then the matrix P_2 is called an M-matrix.

Lemma 4 ([46])**.** Assume $M \in \mathbb{R}^{a \times a}$ is a matrix with positive diagonal elements and non-positive off-diagonal elements. If M is diagonally dominant, then M is an M-matrix.

Lemma 5 (Converse Lyapunov lemma [48])**.** Suppose the LTV system $\dot{x} = A(t)x$ is a globally exponentially stable, where $A(t) : \mathbb{R}^{\geqslant 0} \to \mathbb{R}^{a \times a}$ is a bounded and continuous time-varying matrix. Let $Q_0(t) \in \mathbb{R}^{a \times a}$ be a positive definite time-varying matrix which satisfies $0 < m_3 I < Q_0(t) < m_4 I$, $\forall t \geqslant 0$ with m_3 and m_4 being positive constants. Then there exist positive constants m_1, m_2 such that $0 < m_1 I < P_0(t) < m_2 I$, $\forall t \geqslant 0$, in which $P_0(t) \in \mathbb{R}^{a \times a}$ denotes the unique solution of the following equation:

$$\begin{cases} \dot{P}_0(t) + A(t)^\top P_0(t) + P_0(t)A(t) = -Q_0(t), \\ P_0(0) = I. \end{cases} \tag{8}$$

Moreover, $V_0(t, x) = x^\top P_0(t) x$ can be regarded as a Lyapunov function of the system $\dot{x} = A(t)x$.

3 Cooperative adaptive neural identification

This section is intended to construct NN identifiers with dynamic event-triggered cooperative learning laws for all agents under a directed connected communication topology graph. The stability of the entire identification error system is guaranteed and the Zeno phenomenon is excluded successfully.

For the i-th ($i \in \mathcal{N}$) agent, using the universal approximation ability of RBF NNs, the unknown system dynamics $h_j(\xi_i)$, $j \in \bar{n} = \{1, 2, \ldots, n\}$ can be approximated as follows:

$$h_j(\xi_i) = W_j^{*\top} \Phi_j(\xi_i) + \varepsilon_j'(\xi_i), \tag{9}$$

where $W_j^* \in \mathbb{R}^{l_j}$ is the ideal/optimal weight vector, l_j means the number of NN nodes, and $|\varepsilon_j'(\xi_i)| \leqslant \varepsilon_j^*$ denotes the corresponding fitting error with $\varepsilon_j^* > 0$ being an adequate small constant. From (1) and (9), we have

$$\dot{x}_i = \Phi\left(\xi_i(t)\right)^\top W^* + \varepsilon(\xi_i), \tag{10}$$

where

$$\begin{aligned} W^* &= \left[W_1^{*\top}, W_2^{*\top}, \ldots, W_n^{*\top}\right]^\top, \quad \varepsilon(\xi_i) = \left[\varepsilon_1'(\xi_i), \varepsilon_2'(\xi_i), \ldots, \varepsilon_n'(\xi_i)\right]^\top, \\ \Phi\left(\xi_i(t)\right) &= \operatorname{diag}\left\{\Phi_1(\xi_i(t)), \Phi_2(\xi_i(t)), \ldots, \Phi_n(\xi_i(t))\right\}. \end{aligned} \tag{11}$$

Note that the ideal/optimal weight vector W_j^* is unknown. For agent i, let $\hat{W}_{i,j}$ be employed to estimate W_j^*. Subsequently, the following NN identifier is constructed for agent i

$$\dot{\hat{x}}_i = -K_i\left(\hat{x}_i - x_i\right) + \Phi(\xi_i)^\top \hat{W}_i, \tag{12}$$

where $\hat{x}_i \in \mathbb{R}^n$ is the state estimate vector, $K_i = \operatorname{diag}\left\{k_{i1}, k_{i2}, \ldots, k_{in}\right\}$ is a designed gain matrix with $k_{ij} > 0$, $j \in \bar{n}$, and

$$\hat{W}_i = \left[\hat{W}_{i1}^\top, \hat{W}_{i2}^\top, \ldots, \hat{W}_{in}^\top\right]^\top. \tag{13}$$

Then, the NN weight updating laws are taken as

$$\dot{\hat{W}}_i = -\Gamma_i\left(\Phi(\xi_i)\tilde{x}_i + \sigma_i \hat{W}_i\right) - \tau_i \Gamma_i \sum_{j=1}^{N} a_{ij}\left(\hat{W}_i(t_{k_i}^i) - \hat{W}_j(t_{k_j}^j)\right), \tag{14}$$

where $\tilde{x}_i = \hat{x}_i - x_i = [\tilde{x}_{i1}, \tilde{x}_{i2}, \ldots, \tilde{x}_{in}]^\top$ is the state estimate error vector, $\Gamma_i > 0$ is a positive definite diagonal matrix, a_{ij} is the (i, j) element of the adjacency matrix A corresponding to graph $\mathcal{G}$, $\sigma_i > 0$ is a small constant, $\tau_i > 0$ is a design parameter, and $\hat{W}_i(t_{k_i}^i)$, $i \in \mathbb{N}$ is the latest transmitted NN weights via dynamic event-triggered communication. It is worth pointing out that the transmitted NN weights $\hat{W}_i(t_{k_i}^i)$ remain unchanged in the event-triggering interval $[t_{k_i}^i, t_{k_i+1}^i)$ with $k_i \in \mathbb{N}$. $-\tau_i\Gamma_i \sum_{j=1}^N a_{ij}(\hat{W}_i(t_{k_i}^i) - \hat{W}_j(t_{k_j}^j))$ denotes the cooperative learning term between different agents.

Next, a dynamic event-triggered mechanism is introduced to the communication between adjacent agents. For the i-th agent, we define the following NN weight triggering errors:

$$\delta_{wi}(t) = \hat{W}_i(t_{k_i}^i) - \hat{W}_i(t), \ t \in [t_{k_i}^i, t_{k_i+1}^i), \tag{15}$$

which means the difference between the latest transmitted NN weights $\hat{W}_i(t_{k_i}^i)$ and the current real values $\hat{W}_i(t)$. Define the triggering function for the i-th agent as follows:

$$F_i(t, \eta_i(t), \delta_{wi}(t)) = \eta_i(t) + \theta(c_0 + c_1 \mathrm{e}^{-\rho t} - \|\delta_{wi}(t)\|^2), \tag{16}$$

where $\theta \geqslant 0$, $c_0 > 0$, $c_1 \geqslant 0$, $\rho > 0$ are the design parameters, and $\eta_i(t)$ is the internal dynamic variable with the following updating law:

$$\dot{\eta}_i = -\alpha(\eta_i) + c_0 + c_1 \mathrm{e}^{-\rho t} - \|\delta_{wi}(t)\|^2, \quad \eta_i(0) = \eta_{i0}, \tag{17}$$

where $\alpha(\cdot)$ is a locally Lipschitz continuous $\mathcal{K}_\infty$ function, and η_{i0} is a positive constant. Thus, η_i can be regarded as a filter variable with input $c_0 + c_1\mathrm{e}^{-\rho t} - \|\delta_{wi}(t)\|^2$. Subsequently, consider the following event-triggered rule:

$$\begin{cases} t_0^i = 0, \\ t_{k_i+1}^i = \inf\left\{t \in \mathbb{R} : t > t_{k_i}^i \wedge F_i(t, \eta_i(t), \delta_{wi}(t^-)) \leqslant 0\right\}, \end{cases} \tag{18}$$

where $0 = t_0^i < t_1^i < \cdots < t_{k_i}^i < t_{k_i+1}^i < \cdots$ denotes the triggering time sequence of the i-th agent. In the triggering time $t_{k_i}^i$, we have $\delta_{wi} = 0$.

Next, we present the following lemma to demonstrate that the internal dynamic variables $\eta_i(t),\ i \in \mathcal{N}$, are nonnegative and ultimately bounded. This is of great significance for the reduction of trigger times, stability analysis, and convergence verification for the NN weight estimates.

Lemma 6. Let $\delta_{wi}(t)$ and η_i be given by (15) and (17). Assume $\alpha(\cdot)$ is a locally Lipschitz continuous $\mathcal{K}_\infty$ function and $\eta_{i0} > 0$. Consider the event-triggered rule (18), and then we have $\eta_i(t) + \theta(c_0 + c_1 \mathrm{e}^{-\rho t} - \|\delta_{wi}(t)\|^2) \geqslant 0$ and $\eta_i(t) \geqslant 0$ for all $t \geqslant 0$. Further, η_i is bounded. Moreover, for any constant $s_i > \alpha^{-1}(c_0)$, there exist finite times T_{s_i} and $T_{\eta_i} > T_{s_i}$ such that $\alpha^{-1}(c_0 + c_1 \mathrm{e}^{-\rho T_{s_i}}) < s_i,\ \forall t \geqslant T_{s_i}$ and $|\eta_i(t)| \leqslant s_i,\ \forall t \geqslant T_{\eta_i}$.

Proof. Consider $\|\delta_{wi}(t)\| \leqslant \|\delta_{wi}(t^-)\|$ and the event-triggered rule (18), we have $\eta_i(t) + \theta(c_0 + c_1 \mathrm{e}^{-\rho t} - \|\delta_{wi}(t)\|^2) \geqslant 0$. If $\theta = 0$, then we have $\eta_i(t) \geqslant 0$. If $\theta > 0$, then we have $\dot{\eta}_i \geqslant -\alpha(\eta_i) - \frac{1}{\theta}\eta_i$ by the updating law (17). Noting that η_{i0} is a positive constant, we have $\eta_i(t) \geqslant 0,\ \forall t \geqslant 0$. Consider the updating law (17), we obtain

$$\dot{\eta}_i \leqslant -\alpha(\eta_i) + c_0 + c_1 \mathrm{e}^{-\rho T_{\eta_i}},\ \forall t \geqslant T_{\eta_i}. \tag{19}$$

Since $\alpha(\cdot)$ is a locally Lipschitz continuous $\mathcal{K}_\infty$ function, it is clear that

$$\begin{aligned} &|\eta_i(t)| \leqslant \max\{|\eta_i(0)|,\ \alpha^{-1}(c_0 + c_1)\},\ \forall t \geqslant 0, \\ &|\eta_i(t)| \leqslant s_i,\ \forall t \geqslant T_{\eta_i}, \end{aligned} \tag{20}$$

by the comparison lemma [46, Lemma 3.4].

Remark 2. According to the event-triggered rule (18), each agent transmits its weight estimates to its neighbors only when the weight triggering error norm $\|\delta_{wi}(t)\|^2$ exceeds the time-varying threshold $\eta_i(t)/\theta + c_0 + c_1 \mathrm{e}^{-\rho t}$, which dynamically evolves based on the value of $\eta_i(t)$. Lemma 6 shows that $\eta_i(t)$ remains nonnegative, implying that the term $\eta_i(t)/\theta$ effectively increases the event-triggered threshold compared to the threshold $c_0 + c_1 \mathrm{e}^{-\rho t}$ [37, 38]. Notably, when $\theta \to \infty$, the dynamic event-triggered rule (18) degenerates into the static event-triggered rule proposed in [37, 38]. Furthermore, Lemma 6 indicates that the parameter s_i can be made small by selecting a small c_0 and a large T_{η_i}. It is worth noting that the dynamic event-triggering behavior exhibits distinct behaviors during the transient and steady-state phases of cooperative learning. During the transient phase, agents have not yet fully learned their local dynamics, making the exchange of weight estimates relatively inefficient. Since the dynamic variable $\eta_i(t)$ is initialized with a positive constant, it is guaranteed that $\eta_i(t)$ does not remain zero during this phase. From (17), it can be observed that $\eta_i(t)$ decreases rapidly when $\|\delta_{wi}(t)\|$ becomes large, reflecting an adaptive adjustment mechanism. Conversely, at each triggering instant, $\|\delta_{wi}(t)\|$ is reset to zero, which subsequently leads to an increase in $\eta_i(t)$. In the steady-state phase, the NN weight estimates converge, and the triggering error $\delta_{wi}(t)$ diminishes. Consequently, the growth of $\eta_i(t)$ plateaus and remains below a relatively small value.

The following theorem indicates that the stability of the identification error system (21) is guaranteed and the Zeno phenomenon is avoided successfully.

Theorem 1. Under Assumptions 1 and 2, consider the adaptive identification systems consisting of the N-agent system (1), NN identifiers (12), cooperative NN weight updating laws (14) with the event-triggered rule (18), and the internal variable updating law (17). For the initial conditions satisfying $\hat{W}_i = 0$ and $\eta_i(0) > 0,\ i \in \mathcal{N}$, then we can conclude that

(1) All signals of the adaptive identification systems remain bounded, and the state estimate errors $\tilde{x}_i,\ i \in \mathcal{N}$ can converge to a small neighborhood of the origin within a finite time T;

(2) There exists a positive lower bound on the event-triggered intervals $t_{k_i+1}^i - t_{k_i}^i$ of each agent, which implies that the Zeno phenomenon can be excluded.

Proof. (i) From (10), (12), (14), and (15), we have the identification error systems consisting of the state estimate error subsystems and weight estimate error subsystems:

$$\begin{aligned} \dot{\tilde{x}}_i =& -K_i \tilde{x}_i + \Phi(\xi_i)^\top \tilde{W}_i - \varepsilon(\xi_i), \\ \dot{\tilde{W}}_i =& -\Gamma_i(\Phi(\xi_i)\tilde{x}_i - \sigma_i \hat{W}_i) - \tau_i \Gamma_i \sum_{j=1}^N a_{ij}(\tilde{W}_i - \tilde{W}_j + \delta_{wi} - \delta_{wj}) \end{aligned} \tag{21}$$

with $\tilde{W}_i = \hat{W}_i - W^*$. Then, a parametric Lyapunov function candidate is considered as follows:

$$V = \sum_{i=1}^N \frac{1}{2} d_i \tilde{x}_i^\top \tilde{x}_i + \sum_{i=1}^N \frac{1}{2} d_i \tilde{W}_i^\top \Gamma_i^{-1} \tilde{W}_i, \tag{22}$$

where $d_i > 0$, $i \in \mathcal{N}$, are weighting parameters to be specified later. The time derivative of (22) along system (21) is given by

$$\begin{aligned}\dot{V} =& \sum_{i=1}^{N} d_i \tilde{x}_i^\top \left(-K_i \tilde{x}_i + \Phi\left(\xi_i(t)\right)^\top \tilde{W}_i - \varepsilon_i\right) - \sum_{i=1}^{N} d_i \tilde{W}_i^\top \left(\Phi(\xi_i)\tilde{x}_i + \sigma_i \hat{W}_i\right) \\ & - \sum_{i=1}^{N} \tau_i d_i \tilde{W}_i^\top \sum_{j=1}^{N} a_{ij} \left(\tilde{W}_i - \tilde{W}_j + \delta_{wi} - \delta_{wj}\right) \\ =& - \sum_{i=1}^{N} d_i \tilde{x}_i^\top K_i \tilde{x}_i - \sum_{i=1}^{N} \left(d_i \tilde{x}_i^\top \varepsilon_i + d_i \sigma_i \tilde{W}_i^\top \hat{W}_i\right) \\ & - \sum_{i=1}^{N} d_i \tilde{W}_i^\top \tau_i \sum_{j=1}^{N} a_{ij} \left(\tilde{W}_i - \tilde{W}_j\right) - \tilde{W}^\top \tau D(L \otimes I_l)\delta_w,\end{aligned} \tag{23}$$

where $\varepsilon_i := \varepsilon(\xi_i)$, $l = \sum_{j=1}^{n} l_j$, $\tau = \mathrm{diag}\{\tau_1 I_l, \tau_2 I_l, \ldots, \tau_N I_l\}$, $D = \mathrm{diag}\{d_1 I_l, d_2 I_l, \ldots, d_N I_l\}$, $\tilde{W} = [\tilde{W}_1^\top, \tilde{W}_2^\top, \ldots, \tilde{W}_N^\top]^\top$, and $\delta_w = [\delta_{w1}^\top, \delta_{w2}^\top, \ldots, \delta_{wN}^\top]^\top$. According to the Young's inequality, we have

$$\begin{aligned}&\tilde{x}_i^\top \varepsilon_i \leqslant \frac{\underline{k}}{2} \tilde{x}_i^\top \tilde{x}_i + \frac{1}{2\underline{k}} \bar{\varepsilon}_i, \quad - \tilde{W}_i^\top \hat{W}_i \leqslant -\frac{1}{2} \tilde{W}_i^\top \tilde{W}_i + \frac{1}{2} \left\|W^*\right\|^2, \\ &- \tilde{W}^\top \tau D(L \otimes I_l)\delta_w \leqslant \frac{\mu}{2} \tilde{W}^\top \tilde{W} + \frac{\tau_{\max}^2 d_{\max}^2}{2\mu} \delta_w^\top (L \otimes I_l)^\top (L \otimes I_l)\delta_w,\end{aligned} \tag{24}$$

where $\underline{k} = \min\{k_{11}, k_{12}, \ldots, k_{N,n-1}, k_{Nn}\}$, $\bar{\varepsilon}_i > 0$ is an adequately small constant satisfying $\left\|\varepsilon_i\right\|^2 \leqslant \bar{\varepsilon}_i$, $\mu > 0$ is a design constant, $\tau_{\max} = \max\{\tau_1, \tau_2, \ldots, \tau_N\}$, and $d_{\max} = \max\{d_1, d_2, \ldots, d_N\}$. From (23) and (24), it can be obtained that

$$\begin{aligned}\dot{V} \leqslant& - \frac{\underline{k}}{2} \sum_{i=1}^{N} d_i \tilde{x}_i^\top \tilde{x}_i + \frac{1}{2\underline{k}} \sum_{i=1}^{N} d_i \bar{\varepsilon}_i + \sum_{i=1}^{N} \frac{d_i \sigma_i}{2} \left\|W^*\right\|^2 + \frac{\mu}{2} \tilde{W}^\top \tilde{W} \\ & - \sum_{i=1}^{N} \left[\frac{d_i \sigma_i}{2} \tilde{W}_i^\top \tilde{W}_i + d_i \tau_i \sum_{j=1}^{N} a_{ij} \tilde{W}_i^\top \left(\tilde{W}_i - \tilde{W}_j\right)\right] + \frac{\tau_{\max}^2 d_{\max}^2}{2\mu} \delta_w^\top (L \otimes I_l)^\top (L \otimes I_l)\delta_w \\ =& - \frac{\underline{k}}{2} \sum_{i=1}^{N} d_i \tilde{x}_i^\top \tilde{x}_i - \frac{1}{2} \tilde{W}^\top \left(DP + P^\top D - \mu I_{Nl}\right) \tilde{W} \\ & + \frac{\tau_{\max}^2 d_{\max}^2}{2\mu} \delta_w^\top (L \otimes I_l)^\top (L \otimes I_l)\delta_w + \frac{1}{2\underline{k}} \sum_{i=1}^{N} d_i \bar{\varepsilon}_i + \sum_{i=1}^{N} \frac{d_i \sigma_i}{2} \left\|W^*\right\|^2,\end{aligned} \tag{25}$$

where $P \in R^{Nl \times Nl}$ denotes a block matrix, and the (i,j)-th block matrix P_{ij}, $i, j \in \mathcal{N}$, is given by

$$P_{ij} = \begin{cases} \left(\dfrac{\sigma_i}{2} + \tau_i \sum\limits_{j=1}^{N} a_{ij}\right) I_l, \ i = j, \\ -\tau_i a_{ij} I_l, \ i \neq j. \end{cases} \tag{26}$$

It is clear from (26) that P is a diagonally dominant matrix, whose all diagonal elements and off-diagonal elements are positive and non-positive, respectively. Based on Lemma 4, we have P is an M-matrix. Furthermore, based on Lemma 3, we can choose d_i, $i \in \mathcal{N}$ such that $DP + P^\top D = Q$ with $Q > 0$ being a positive definite matrix. In this way, from (25), it follows

$$\begin{aligned}\dot{V} \leqslant& - \frac{\underline{k}}{2} \sum_{i=1}^{N} d_i \tilde{x}_i^\top \tilde{x}_i - \frac{1}{2} \tilde{W}^\top \left(Q - \mu I_{Nl}\right) \tilde{W} + \frac{\tau_{\max}^2 d_{\max}^2 \lambda_L}{2\mu} \left\|\delta_w\right\|^2 + \varrho \\ \leqslant& - \frac{\underline{k} d_{\min}}{2} \tilde{x}^\top \tilde{x} - \frac{\lambda_{\min}(Q) - \mu}{2} \tilde{W}^\top \tilde{W} + \frac{\tau_{\max}^2 d_{\max}^2 \lambda_L}{2\mu} \left\|\delta_w\right\|^2 + \varrho,\end{aligned} \tag{27}$$

where $d_{\min} = \min\{d_1, d_2, \ldots, d_N\}$, $\tilde{x} = \left[\tilde{x}_1^\top, \tilde{x}_2^\top, \ldots, \tilde{x}_N^\top\right]^\top$, $\varrho = \frac{1}{2\underline{k}}\sum_{i=1}^N d_i\bar{\varepsilon}_i + \sum_{i=1}^N \frac{d_i\sigma_i}{2}\|W^*\|^2$, and $\lambda_L = \lambda_{\max}\left((L\otimes I_l)^\top(L\otimes I_l)\right)$. Based on (17), (18), and Lemma 6, it can be concluded that the inequality $\|\delta_{wi}\|^2 \leqslant \frac{s_i}{\theta} + c_0 + c_1 \mathrm{e}^{-\rho T_{\eta_i}}$ holds for all $t > T_{\eta_i}$. Define $T_\eta = \max\{T_{\eta_1}, T_{\eta_2}, \ldots, T_{\eta_N}\}$ and $s = \max\{s_1, s_2, \ldots, s_N\}$, and then we have $\|\delta_w\|^2 \leqslant \frac{Ns}{\theta} + Nc_0 + c_1\sum_{i=1}^N \mathrm{e}^{-\rho T_{\eta_i}}$, $\forall t > T_\eta$. Recalling (27), we have

$$\dot{V} \leqslant -\frac{\underline{k}d_{\min}}{2}\tilde{x}^\top\tilde{x} - \frac{\lambda_{\min}(Q)-\mu}{2}\tilde{W}^\top\tilde{W} + \varrho', \ \forall t > T_\eta \tag{28}$$

with $\varrho' = \frac{Ns}{\theta} + Nc_0 + c_1\sum_{i=1}^N \mathrm{e}^{-\rho T_{\eta_i}} + \varrho$. Furthermore, we can design μ such that $\mu < \lambda_{\min}(Q)$. In this way, there exists a finite time $T > T_\eta$, such that

$$\|\tilde{x}\| \leqslant \frac{2\varrho_1'}{\underline{k}d_{\min}}, \quad \|\tilde{W}\| \leqslant \frac{2\varrho_1'}{\lambda_{\min}(Q)-\mu}, \quad \forall t > T \tag{29}$$

with $\varrho_1' > \varrho'$, which indicates that identification errors $\|\tilde{x}\|$ and $\|\tilde{W}\|$ are ultimately bounded. Furthermore, we can choose a large θ, small c_0, large T_{η_i}, small σ_i, and large $\underline{k}$, such that $\frac{2\varrho_1'}{\underline{k}d_{\min}}$ is small enough, that is, the state estimate errors $\tilde{x}_i$ can converge to a small neighborhood of the origin in $t > T$. Note that $\alpha(\cdot)$ belongs to $\mathcal{K}_\infty$ functions, and then it is clear that η_i, $i \in \mathcal{N}$ remain bounded in $t > 0$ by (17). Let $\eta_i \leqslant \bar{\eta}_i$, $i \in \mathcal{N}$ with constant $\bar{\eta}_i > 0$. According to the event-triggered rule (18), it is easy to obtain that $\|\delta_{wi}\|^2 \leqslant \frac{\eta_i}{\theta} + c_0 + c_1$, $\forall t > 0$ holds. Subsequently, it is clear from (27) that $\|\tilde{x}\|$ and $\|\tilde{W}\|$ are bounded in $t \geqslant 0$. Since x_i, $i \in \mathcal{N}$, and W_j^*, $j \in \bar{n}$ are bounded, then we have the system state and NN weight estimates $\hat{x}_i$, $\hat{W}_{ij}$, $i \in \mathcal{N}$, $j \in \bar{n}$ are also bounded.

(ii) To exclude the Zeno phenomenon, it is necessary to demonstrate the existence of a positive lower bound for the inter-event intervals. From (18), we have $\delta_{wi}(t_{k_i}^i) = 0$. In the triggering interval $[t_{k_i}^i, t_{k_i+1}^i)$, it follows that $\delta_{wi} = \dot{\hat{W}}_i = \chi_i$, where $\chi_i = -\Gamma_i(\Phi(\xi_i)\tilde{x}_i + \sigma_i\hat{W}_i) - \tau_i\Gamma_i\sum_{j=1}^N a_{ij}(\hat{W}_i(t_{k_i}^i) - \hat{W}_j(t_{k_j}^j))$. Thus, we have

$$\|\delta_{wi}\| \leqslant \int_{t_{k_i}^i}^t \|\chi_i\|\,dt, \ t \in [t_{k_i}^i, t_{k_i+1}^i). \tag{30}$$

Next, we verify the boundedness of $\|\chi_i\|$. Note that $\|\tilde{x}_i\|$ and $\|\hat{W}_i\|$ are bounded, and thus there exist positive constants $\kappa_x > 0$, $\kappa_w > 0$ such that $\|\tilde{x}_i\| \leqslant \kappa_x$ and $\|\hat{W}_i\| \leqslant \kappa_w$. Therefore, it is easy to obtain

$$\|\chi_i\| \leqslant \|\Gamma_i\|\left[l\kappa_x + \sigma_i\kappa_w + 2\tau_i N_i\kappa_w\right] =: \bar{\chi}_i, \tag{31}$$

where N_i denotes the number of neighbors of the i-th agent. Consider (30) and (31), and it is clear that $\|e_{wi}\| \leqslant \bar{\chi}_i(t - t_{k_i}^i)$. Therefore, there exists a lower bound $\frac{\sqrt{c_0}}{\bar{\chi}_i}$ for all event-triggered intervals, because the next event will not be triggered before $\|\delta_{wi}\| \geqslant \sqrt{c_0}$.

Remark 3. In [30, 34–38], the Lyapunov function is chosen as $V = \sum_{i=1}^N \frac{1}{2}\tilde{x}_i^\top\tilde{x}_i + \sum_{i=1}^N \frac{1}{2}\tilde{W}_i^\top\Gamma_i^{-1}\tilde{W}_i$, which can be viewed as a special case of the proposed parametric Lyapunov function (22) by setting $d_i = 1$ for all $i \in \mathcal{N}$. In this case, the term $-\frac{1}{2}\tilde{W}^\top(DP + P^\top D - \mu I_{Nl})\tilde{W}$ reduces to $-\frac{1}{2}\tilde{W}^\top(P + P^\top - \mu I_{Nl})\tilde{W}$, which can be interpreted as an interactive perturbation introduced by the cooperative learning term $-\tau_i\Gamma_i\sum_{j=1}^N a_{ij}(\hat{W}_i(t_{k_i}^i) - \hat{W}_j(t_{k_j}^j))$ in the NN weight updating law (14), thereby complicating the stability analysis. For undirected graphs, it follows directly from (26) that P is positive definite, implying that $P + P^\top$ is also positive definite. However, for directed graphs, P is neither symmetric nor positive definite, which introduces significant challenges in analyzing the closed-loop stability. By recognizing P as a nonsingular M-matrix, a parameterized Lyapunov function is constructed, and the properties of M-matrices are utilized to ensure that $DP + P^\top D$ remains positive definite. As shown in (26), the matrix P_l, $l \in \bar{n}$, is diagonally dominant, which guarantees that P_l qualifies as an M-matrix. This property is crucial for the validity of the proposed M-matrix-based parameterized Lyapunov function. From a system-theoretic perspective, the cooperative learning term embedded in the NN weight update law introduces an external perturbation to each agent's individual tracking task. The matrix P_l encodes the inter-agent coupling dynamics: its diagonal elements reflect the "degree of stability" of each isolated agent, while the off-diagonal elements quantify the "strength of interconnection" among agents. The M-matrix property of P_l ensures that the "degree of stability" dominates the "strength of interconnection", thereby guaranteeing both the overall multi-agent closed-loop stability and individual identification performance. The stability analysis of Theorem 1 can be completed by selecting the weighting parameters d_i, $i \in \mathcal{N}$ suitably based on Lemma 3. It is worth noting that the weighting parameters

$d_i,\ i\in\mathcal{N}$ in the proposed parameterized Lyapunov function are used solely for stability analysis and do not appear in the cooperative adaptive neural identifier design, as detailed in (12), (14), (17), and (18). Consequently, there is no need to select or tune weighting parameters $d_i,\ i\in\mathcal{N}$ in practical implementation. Meanwhile, from the explicit expression of P_{ij} given in (26), the values of $d_i,\ i\in\mathcal{N}$ depend on σ_i, τ_i, and the inter-agent communication topology $\mathcal{G}$. $d_i,\ i\in\mathcal{N}$ are directly determined by P, and their specific values can be referred to [49, 50]. Moreover, the state estimate error $\tilde{x}_i$ can converge to a small neighborhood of the origin within a finite time T, which is essential for the successful implementation of DCL in the subsequent section.

4 Knowledge acquisition and storage

This section presents the knowledge acquisition and storage regarding the unknown system dynamics $H(\cdot)$. RBF NNs will be verified to achieve accurate approximation for the unknown dynamics $h_j(\cdot)$, $j\in\bar{n}$ along the union of system trajectories of all agents. To this end, it is necessary to construct the dynamic equations related to the NN weight estimate errors of all agents and further prove that it can converge to a small neighborhood of the origin. Since the exponential convergence results for specific linear time-varying (LTV) systems [29] are subject to undirected topology graphs, the existing exponential convergence results are no longer applicable. Hence, we propose a group-convergence-proof strategy, integrating the converse Lyapunov lemma and the directed trees lemma, to achieve the convergence results of NN weight estimates.

For simplicity, the related notations are provided in advance:

(1) $\varphi(\xi_i(t)),\ i\in\mathcal{N}$ denotes the system trajectory of the i-th agent;

(2) $\varphi(\xi(t))$ signifies the union trajectory of N agents, i.e., $\varphi(\xi(t))=\bigcup_{i=1}^{N}\varphi(\xi_i(t))$;

(3) $(\cdot)_{\zeta_i}$ and $(\cdot)_{\bar{\zeta}_i}$ mean the part of $(\cdot)$ corresponding to the region close to and far away from the trajectory of the i-th agent $\varphi(\xi_i(t))$, respectively;

(4) $(\cdot)_{\zeta}$ and $(\cdot)_{\bar{\zeta}}$ mean the part of $(\cdot)$ corresponding to the region close to and far away from the union trajectory $\varphi(\xi(t))$, respectively.

The following theorem shows the convergence of NN weight estimates, and the unknown system dynamics can be accurately identified by the two RBF NNs $\hat{W}_{i,j}\Phi_j(\xi)$ and $\bar{W}_{i,j}\Phi_j(\xi)$, where constant weights $\bar{W}_{i,j}$ are given in (32).

Theorem 2. Under Assumptions 1 and 2, consider the adaptive identification systems consisting of N agents (1), neural identifiers (12), cooperative neural weights updating laws (14) with event-triggered rules (18), and internal dynamic variable updating laws (17). Let the initial conditions satisfy $\hat{W}_i=0$ and $\eta_i(0)>0$ for all $i\in\mathcal{N}$. Then, we have

(1) The NN weight estimates $\hat{W}_{i,\zeta}$ of all agents converge uniformly exponentially to a small neighborhood of their common ideal weights W_{ζ}^{*} by appropriately choosing design parameters;

(2) The unknown system functions $h_j(\xi)$, $j\in\bar{n}$ can be accurately identified by the two RBF NNs $\hat{W}_{i,j}\Phi_j(\xi)$ and $\bar{W}_{i,j}\Phi_j(\xi)$ along the union trajectory $\varphi(\xi(t))$, where

$$\bar{W}_{i,j}=\underset{t\in[t_a,t_b]}{\text{mean}}\,\hat{W}_{i,j}(t)=\frac{1}{t_b-t_a}\int_{t_a}^{t_b}\hat{W}_{i,j}(s)ds \tag{32}$$

with $[t_a,t_b],\ T<t_a<t_b$ being a time interval after the transient-state process.

Proof. System (21) can be rewritten as

$$\begin{aligned}\dot{\tilde{x}}_i=&-K_i\tilde{x}_i+\Phi_{\zeta}\left(\xi_i(t)\right)^{\top}\tilde{W}_{i\zeta}-\varepsilon_{i\zeta},\\ \dot{\tilde{W}}_{i\zeta}=&-\Gamma_{i\zeta}\left(\Phi_{\zeta}\left(\xi_i\right)\tilde{x}_i+\sigma_i\hat{W}_{i\zeta}\right)-\tau_i\Gamma_{i\zeta}\sum_{j=1}^{N}a_{ij}\left(\tilde{W}_{i\zeta}-\tilde{W}_{j\zeta}+\delta_{wi\zeta}-\delta_{wj\zeta}\right)\end{aligned} \tag{33}$$

with $i\in\mathcal{N}$ and $\varepsilon_{i\zeta}=\varepsilon(\xi_i)-\tilde{W}_{i\bar{\zeta}}^{\top}\Phi_{\bar{\zeta}}(\xi_i)$. Then, we can rewrite (33) in the following compact form:

$$\begin{bmatrix}\dot{\tilde{x}}\\ \dot{\tilde{W}}_{\zeta}\end{bmatrix}=\begin{bmatrix}K & \Psi_{\zeta}(t)^{\top}\\ -\Gamma_{\zeta}\Psi_{\zeta}(t) & -\tau_{\zeta}\Gamma_{\zeta}\left(L\otimes I_{l_{\zeta}}\right)\end{bmatrix}\begin{bmatrix}\tilde{x}\\ \tilde{W}_{\zeta}\end{bmatrix}+\begin{bmatrix}-\bar{\varepsilon}_{\zeta}\\ -\Gamma_{\zeta}\Lambda_{\zeta}\hat{W}_{\zeta}-\tau_{\zeta}\Gamma_{\zeta}\left(L\otimes I_{l_{\zeta}}\right)\delta_{w\zeta}\end{bmatrix}, \tag{34}$$

where $l_{\zeta}=\sum_{j=1}^{n}l_{j\zeta}$ with $l_{j\zeta}$ being the number of NN nodes close to the union trajectory $\varphi(\xi(t))$ with respect to

$\Phi_j(\cdot)$,

$$\begin{aligned}
&\tilde{W}_\zeta = \left[\tilde{W}_{1\zeta}^\top, \ldots, \tilde{W}_{N\zeta}^\top\right]^\top, \qquad \hat{W}_\zeta = \left[\hat{W}_{1\zeta}^\top, \ldots, \hat{W}_{N\zeta}^\top\right]^\top,\\
&\delta_{w\zeta} = \left[\delta_{w1\zeta}^\top, \delta_{w2\zeta}^\top, \ldots, \delta_{wN\zeta}^\top\right]^\top, \quad \bar{\varepsilon}_\zeta = \left[\varepsilon_{1\zeta}^\top, \varepsilon_{2\zeta}^\top \ldots, \varepsilon_{N\zeta}^\top\right]^\top,\\
&\Gamma_\zeta = \operatorname{diag}\left\{\Gamma_{1\zeta}, \ldots, \Gamma_{N\zeta}\right\}, \qquad \Lambda_\zeta = \operatorname{diag}\left\{\sigma_1 I_{l_\zeta}, \ldots, \sigma_N I_{l_\zeta}\right\},\\
&K = \operatorname{diag}\left\{-K_1, \ldots, -K_N\right\}, \qquad \tau_\zeta = \operatorname{diag}\left\{\tau_1 I_{l_\zeta}, \ldots, \tau_N I_{l_\zeta}\right\},\\
&\Psi_\zeta(t) = \operatorname{diag}\left\{\Phi_\zeta\left(\xi_1(t)\right), \Phi_\zeta\left(\xi_2(t)\right), \ldots, \Phi_\zeta\left(\xi_N(t)\right)\right\}.
\end{aligned} \tag{35}$$

Next, we will show exponential convergence of the normal part of system (34). A novel group-convergence-proof strategy is given as follows. Note that $\tilde{W}_{i\zeta} = \tilde{W}_{i\zeta_1} \cup \tilde{W}_{i\zeta_2} \cup \cdots \cup \tilde{W}_{i\zeta_N}$, $i \in \mathcal{N}$, and thus the convergence verification of (34) can be converted into the convergence verification of N groups $\{\tilde{x}_i, \tilde{W}_{1\zeta_i}, \tilde{W}_{2\zeta_i}, \ldots, \tilde{W}_{N\zeta_i}\}$, $i \in \mathcal{N}$. The convergence of $\{\tilde{x}_1, \tilde{W}_{1\zeta_1}, \tilde{W}_{2\zeta_1}, \ldots, \tilde{W}_{N\zeta_1}\}$ is firstly verified. From system (33), we can immediately obtain (36), where $\varepsilon_{1\zeta_1} = \varepsilon(\xi_1) - \tilde{W}_{1\bar{\zeta}_1}^\top \Phi_{\bar{\zeta}_1}(\xi_1)$ remains small.

$$\begin{aligned}
\begin{bmatrix} \dot{\tilde{x}}_1 \\ \dot{\tilde{W}}_{1\zeta_1} \\ \dot{\tilde{W}}_{2\zeta_1} \\ \vdots \\ \dot{\tilde{W}}_{N\zeta_1} \end{bmatrix} &= \begin{bmatrix} -K_1 & \Phi_{\zeta_1}\left(\xi_1(t)\right)^\top & 0 & \cdots & 0 \\ -\Gamma_{1\zeta_1}\Phi_{\zeta_1}\left(\xi_1(t)\right) & -\tau_1\Gamma_{1\zeta_1}\sum_{j=1}^N a_{1j} & \tau_1\Gamma_{1\zeta_1}a_{12} & \cdots & \tau_1\Gamma_{1\zeta_1}a_{1N} \\ 0 & \tau_2\Gamma_{2\zeta_1}a_{21} & -\tau_2\Gamma_{2\zeta_1}\sum_{j=1}^N a_{2j} & \cdots & \tau_2\Gamma_{2\zeta_1}a_{2N} \\ \vdots & \vdots & \vdots & \ddots & \vdots \\ 0 & \tau_N\Gamma_{N\zeta_1}a_{N1} & \tau_N\Gamma_{N\zeta_1}a_{N2} & \cdots & -\tau_N\Gamma_{N\zeta_1}\sum_{j=1}^N a_{Nj} \end{bmatrix} \begin{bmatrix} \tilde{x}_1 \\ \tilde{W}_{1\zeta_1} \\ \tilde{W}_{2\zeta_1} \\ \vdots \\ \tilde{W}_{N\zeta_1} \end{bmatrix} \\
&+ \begin{bmatrix} \Phi_{\bar{\zeta}_1}\left(\xi_1\right)^\top \tilde{W}_{1\bar{\zeta}_1} - \varepsilon_{1\zeta_1} \\ -\sigma_1\Gamma_{1\zeta_1}\hat{W}_{1\zeta_1} - \tau_1\Gamma_{1\zeta_1}\sum_{j=1}^N a_{1j}\left(\delta_{w1\zeta_1} - \delta_{wj\zeta_1}\right) \\ -\Gamma_{2\zeta_1}\Phi_{\zeta_1}\left(\xi_2\right)\tilde{x}_2 - \sigma_2\Gamma_{2\zeta_1}\hat{W}_{2\zeta_1} - \tau_2\Gamma_{2\zeta_1}\sum_{j=1}^N a_{2j}\left(\delta_{w2\zeta_1} - \delta_{wj\zeta_1}\right) \\ \vdots \\ -\Gamma_{N\zeta_1}\Phi_{\zeta_1}\left(\xi_N\right)\tilde{x}_N - \sigma_N\Gamma_{N\zeta_1}\hat{W}_{N\zeta_1} - \tau_N\Gamma_{N\zeta_1}\sum_{j=1}^N a_{Nj}\left(\delta_{wN\zeta_1} - \delta_{wj\zeta_1}\right) \end{bmatrix}.
\end{aligned} \tag{36}$$

Let

$$\bar{\Theta} = \left[\Theta_1^{\mathrm{T}}, \Theta_2^{\mathrm{T}}\right]^{\mathrm{T}}, \ \Theta_1 = \begin{bmatrix} \tilde{x}_1^\top & \tilde{W}_{1\zeta_1}^\top \end{bmatrix}^\top, \ \Theta_2 = \begin{bmatrix} \tilde{W}_{2\zeta_1}^\top & \tilde{W}_{3\zeta_1}^\top & \cdots & \tilde{W}_{N\zeta_1}^\top \end{bmatrix}^\top. \tag{37}$$

Let $\mathcal{G}_1$ be a graph with the node set $\mathcal{V}_1 = \{v_2, v_3, \ldots, v_N\}$ and the edge set $\mathcal{E} - \{(v_1, v_j) \mid v_j \in \mathcal{V}_1\} \cup \{(v_j, v_1) \mid v_j \in \mathcal{V}_1\}$. By removing the edges directed towards agent v_1 and designating agent v_1 as the leader, we define H_1 as the leader-following matrix with respect to the graph $\bar{\mathcal{G}}_1$. It is clear that $\bar{\mathcal{G}}_1$ is a directed tree with v_1 being the leader. Subsequently, the normal part of system (36) can be rewritten as

$$\dot{\bar{\Theta}} = \begin{bmatrix} \dot{\Theta}_1 \\ \dot{\Theta}_2 \end{bmatrix} = \left[\begin{array}{c|c} A_1(t) & 0 \\ \hline 0 & -\Pi_1\Upsilon_1\left(H_1 \otimes I_{l_{\zeta_1}}\right) \end{array}\right] \begin{bmatrix} \Theta_1 \\ \Theta_2 \end{bmatrix} + \left[\begin{array}{c|c} B_1 & C_1 \\ \hline D_1 & 0 \end{array}\right] \begin{bmatrix} \Theta_1 \\ \Theta_2 \end{bmatrix}, \tag{38}$$

where

$$\begin{aligned}
&\Pi_1 = \operatorname{diag}\left\{\tau_2 I_{l\zeta_1}, \tau_3 I_{l\zeta_1}, \ldots, \tau_N I_{l\zeta_1}\right\}, \quad \Upsilon_1 = \operatorname{diag}\left\{\Gamma_{2\zeta_1}, \Gamma_{3\zeta_1}, \ldots, \Gamma_{N\zeta_1}\right\},\\
&A_1(t) = \begin{bmatrix} -K_1 & \Phi_{\zeta_1}\left(\xi_1(t)\right)^\top \\ -\Gamma_{1\zeta_1}\Phi_{\zeta_1}\left(\xi_1\right) & 0 \end{bmatrix}, \quad B_1 = \begin{bmatrix} 0 & 0 \\ 0 & -\tau_1\Gamma_{1\zeta_1}\sum_{j=1}^N a_{1j} \end{bmatrix},\\
&C_1 = \begin{bmatrix} 0 & \cdots & 0 \\ \tau_1\Gamma_{1\zeta_1}a_{12} & \cdots & \tau_1\Gamma_{1\zeta_1}a_{1N} \end{bmatrix}, \qquad D_1 = \begin{bmatrix} 0 & \tau_2\Gamma_{2\zeta_1}a_{21} \\ \vdots & \vdots \\ 0 & \tau_N\Gamma_{N\zeta_1}a_{N1} \end{bmatrix},
\end{aligned} \tag{39}$$

and $l_{\zeta_1} = \sum_{j=1}^n l_{j\zeta_1}$, where $l_{j\zeta_1}$ denotes the number of NN nodes in proximity to the trajectory of the first agent $\varphi(\xi_1(t))$ with respect to $\Phi_j(\cdot)$. According to Assumption 1 and Lemma 2, it is clear that $\Phi_{\zeta_1}\left(\xi_1(t)\right)$ is persistently exciting. By Theorem 1 given in [48], we have the LTV system $\dot{\Theta}_1 = A_1(t)\Theta_1$ is globally exponentially stable. Then, we choose the following Lyapunov function candidate:

$$V_l = \bar{\Theta}^\top \begin{bmatrix} \omega P_1(t) & \\ & \left(P_2 \otimes I_{l_{\zeta_1}}\right)\Pi_1^{-1}\Upsilon_1^{-1} \end{bmatrix} \bar{\Theta} = \omega\Theta_1^\top P_1(t)\Theta_1 + \Theta_2^\top\left(P_2 \otimes I_{l\zeta_1}\right)\Pi_1^{-1}\Upsilon_1^{-1}\Theta_2 \tag{40}$$

with the design parameter $\omega > 0$, where $P_1(t)$ and P_2 denote a time-varying positive definite matrix and positive definite diagonal matrix, respectively, such that

$$\begin{cases} \dot{P}_1(t) + A_1(t)^\top P_1(t) + P_1(t)A_1(t) = -Q_1(t), \\ P_2H_1 + H_1^\top P_2 = Q_2, \\ 0 < p_{1m}I \leqslant P_1(t) \leqslant p_{1M}I, \\ 0 < p_{2m}I \leqslant P_2 \leqslant p_{2M}I, \\ 0 < q_{1m}I \leqslant Q_1(t) \leqslant q_{1M}I, \\ 0 < q_{2m}I \leqslant Q_2 \leqslant q_{2M}I, \end{cases} \tag{41}$$

hold by Lemma 1 and Lemma 5. The time derivative of V_l along system (38) is given by

$$\begin{aligned} \dot{V}_l =& \omega \left(A_1(t)\Theta_1 + B_1\Theta_1 + C_1\Theta_2\right)^\top P_1(t)\Theta_1 + \omega\Theta_1^\top \dot{P}_1(t)\Theta_1 \\ &+ \omega\Theta_1^\top P_1(t)\left(A_1(t)\Theta_1 + B_1\Theta_1 + C_1\Theta_2\right) \\ &- \Theta_2^\top \left((P_2H_1 + H_1^\top P_2)\otimes I_{l_{\zeta_1}}\right)\Theta_2 + 2\Theta_1^\top D_1^\top \left(P_2 \otimes I_{l_{\zeta_1}}\right)\Pi_1^{-1}\Upsilon_1^{-1}\Theta_2 \\ =& -\omega\Theta_1^\top Q_1(t)\Theta_1 - \Theta_2^\top \left(Q_2 \otimes I_{l_{\zeta_1}}\right)\Theta_2 + 2\omega\Theta_1^\top P_1(t)B_1\Theta_1 \\ &+ 2\Theta_1^\top \left(D_1^\top \left(P_2 \otimes I_{l_{\zeta_1}}\right)\Pi_1^{-1}\Upsilon_1^{-1} + \omega P_1(t)C_1\right)\Theta_2. \end{aligned} \tag{42}$$

Consider (41) and the Young's equality, and then we have

$$\begin{aligned} &2\omega\Theta_1^\top P_1(t)B_1\Theta_1 \leqslant 2\omega p_{1M}\tau_1\gamma_{1M}N\bar{a}\Theta_1^\top\Theta_1, \\ &2\Theta_1^\top D_1^\top \left(P_2 \otimes I_{l_{\zeta_1}}\right)\Pi_1^{-1}\Upsilon_1^{-1}\Theta_2 \leqslant \frac{l_{\zeta_1}\bar{a}p_{2M}}{c}(N-1)\Theta_1^\top\Theta_1 + cl_{\zeta 1}\bar{a}p_{2M}(N-1)\Theta_2^\top\Theta_2, \\ &2\omega\Theta_1^\top P_1(t)C_1\Theta_2 \leqslant \frac{l_{\zeta_1}\bar{a}}{c}(N-1)p_{1M}\omega^2\tau_1^2\gamma_{1M}^2\Theta_1^\top\Theta_1 + cl_{\zeta_1}\bar{a}(N-1)p_{1M}\Theta_2^\top\Theta_2, \end{aligned} \tag{43}$$

where $\bar{a}$ is the least upper bound of all elements of the adjacency matrix A, $c > 0$ denotes a design parameter, and $\gamma_{1M} = \lambda_{\max}(\Gamma_1)$. By combining (42) and (43), we have

$$\begin{aligned} \dot{V}_l \leqslant& -\left(\omega q_{1m} - 2\omega p_{1M}\tau_1\gamma_{1M}N\bar{a}\right)\Theta_1^\top\Theta_1 - \left(\frac{l_{\zeta_1}\bar{a}}{c}(N-1)\left(p_{2M} + p_{1M}\omega^2\tau_1^2\gamma_{1M}^2\right)\right)\Theta_1^\top\Theta_1 \\ &- \left(q_{2m} - cl_{\zeta 1}\bar{a}(N-1)\left(p_{2M} + p_{1M}\right)\right)\Theta_2^\top\Theta_2. \end{aligned} \tag{44}$$

If the design parameters $c > 0$, $\omega > 0$, and $\tau_1 > 0$ are chosen such that

$$\begin{cases} c < \dfrac{q_{2m} - \beta_2}{l_{\zeta 1}\bar{a}(N-1)\left(p_{2M} + p_{1M}\right)}, \\ \omega > \dfrac{\beta_1 + \beta_3 + \frac{l_{\zeta_1}\bar{a}}{c}(N-1)p_{2M}}{q_{1m}}, \\ 2\omega p_{1M}\tau_1\gamma_{1M}N\bar{a} + \dfrac{l_{\zeta 1}\bar{a}}{c}(N-1)p_{1M}\omega^2\tau_1^2\gamma_{1M}^2 < \beta_3, \end{cases} \tag{45}$$

where $0 < \beta_2 < q_{2m}$ and $\beta_1,\ \beta_3 > 0$, then, we have

$$\dot{V}_l \leqslant -\beta_1\Theta_1^\top\Theta_1 - \beta_2\Theta_2^\top\Theta_2, \tag{46}$$

which indicates the normal part of system (36) is globally exponentially stable. Based on Theorem 1, it is clear that $\tilde{x}_i$ $(i = 2, 3, \ldots, N)$ remains small and $\hat{W}_i$ $(i = 1, 2, \ldots, N)$ is bounded in $t > T$. With a small c_0 and a large T_{η_i}, δ_{wi} is also small for $t > T$. Note $\Phi_{\bar{\zeta}_1}\left(\xi_1\right)^\top \tilde{W}_{1\bar{\zeta}_1}$ remains small because the corresponding NN nodes are far away from the trajectory $\varphi(\xi_1(t))$. Consequently, system (36) for $t > T$ can be regarded as a globally exponentially stable LTV system with a small disturbance term. Therefore, $\{\tilde{x}_1, \tilde{W}_{1\zeta_1}, \tilde{W}_{2\zeta_1}, \ldots, \tilde{W}_{N\zeta_1}\}$ can converge to a close vicinity of the origin for $t > T_1$ with $T_1 > T > 0$. By renumbering all agents and designating the i-th agent υ_i as υ_1, and following a similar procedure, it can be shown that $\{\tilde{x}_i, \tilde{W}_{1\zeta_i}, \tilde{W}_{2\zeta_i}, \ldots, \tilde{W}_{N\zeta_i}\}$ $(i = 2, 3, \ldots, N)$ converges to a small neighborhood of the origin for $t > T_i$ with $T_i > T > 0$. Hence, it can be concluded that the error

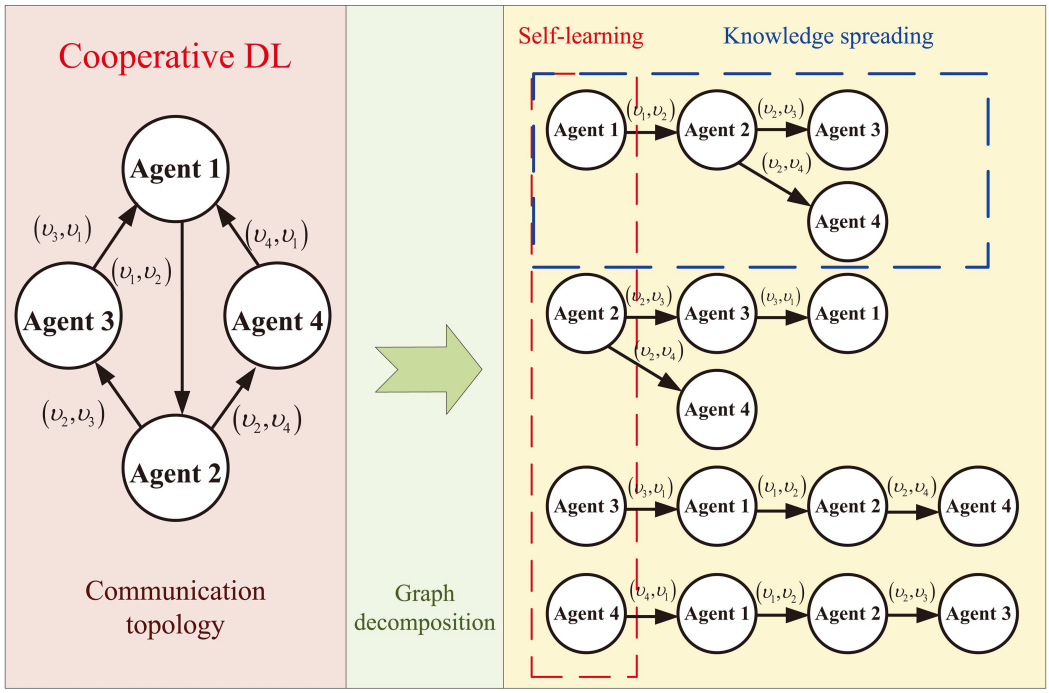

Figure 1 (Color online) Example of graph decomposition involving four agents.

system (34) converges to a small neighborhood of the origin for $t > \bar{T}$, where $\bar{T} = \max\{T_1, T_2, \ldots, T_N\}$. Given that $\tilde{W}_\zeta = \hat{W}_\zeta - 1_N \otimes W_\zeta^*$, it is clear that $\hat{W}_{i\zeta}$ converges to a small neighborhood of W_ζ^* for $i \in \mathcal{N}$. Moreover, along the union trajectory $\varphi(\xi(t))$, we have

$$h_j(\xi) = \hat{W}_{i,j\zeta}^\top \Phi_{j\zeta}(\xi) + \varepsilon''_{j\zeta}(\xi) = \hat{W}_{i,j}^\top \Phi_j(\xi) + \varepsilon''_j(\xi) = \bar{W}_{i,j}^\top \Phi_j(\xi) + \varepsilon'''_j(\xi), \tag{47}$$

where $\varepsilon''_{j\zeta}(\xi)$, $\varepsilon''_j(\xi) = \varepsilon''_{j\zeta}(\xi) - \hat{W}_{i,j\bar{\zeta}}\Phi_{j\bar{\zeta}}(\xi)$, and $\varepsilon'''_j(\xi) = \varepsilon''_j(\xi) + (\hat{W}_{i,j} - \bar{W}_{i,j})\Phi_j(\xi)$ remain small, due to the convergence of $\hat{W}_{i,j}$ and the localized approximation of RBF NNs.

Remark 4. In [30, 34–38], the convergence analysis of system (34) is based on the convergence theory of LTV systems under the cooperative PE condition, as stated in Theorem 1 of [29]. However, Theorem 1 in [29] requires that the term $\tau\Gamma_\zeta(L \otimes I_{l_\zeta})$ appearing in system (34) be positive semi-definite. Since the Laplacian matrix L associated with directed graphs does not possess this property, the convergence analysis of system (34) cannot be directly established using the existing theoretical framework. It has been observed that a directed connected graph can be conceptualized as a combination of directed trees, with each node acting as the root. Consequently, an intuitive strategy is for each agent to independently acquire knowledge along its own trajectory and propagate this knowledge through a directed tree in which it serves as the root node. By employing this graph decomposition approach, the convergence analysis of system (34) can be decomposed into N groups $\{\tilde{x}_i, \tilde{W}_{1\zeta_i}, \tilde{W}_{2\zeta_i}, \ldots, \tilde{W}_{N\zeta_i}\}$, $i \in \mathcal{N}$. Within each group, the root node of the directed tree acts as a virtual leader, thereby transforming the consensus convergence problem of NN weight estimates among agents into two subproblems: an individual learning problem for the virtual leader and a consensus convergence problem for the virtual followers. Following a similar proof procedure as outlined in [16], it can be shown that $\dot{\Theta}_1 = A_1(t)\Theta_1$ is globally exponentially stable due to the PE property of $\Phi_{\zeta_1}(\xi_1(t))$. This demonstrates that each agent is capable of effectively learning the knowledge associated with its own trajectory. Consequently, the Lyapunov function (40) consists of two components: the first term $\omega\Theta_1^\top P_1(t)\Theta_1$ represents the self-learning capability of each agent, while the second term $\Theta_2^\top(P_2 \otimes I_{l\zeta_1})\Pi_1^{-1}\Upsilon_1^{-1}\Theta_2$ captures the knowledge-sharing mechanism among interconnected agents. As illustrated in Figure 1, an example of graph decomposition for DCL involving four agents is presented. The original directed communication topology is decomposed into four directed trees, each containing a virtual leader (i.e., the root node) that performs individual self-learning and disseminates the acquired knowledge to the other agents via the tree structure.

Remark 5. To ensure optimal learning performance under event-triggered communication, the triggering error $\delta_{wi\zeta}$ must remain small for $t > T$, thereby minimizing the disturbance term in (36). According to Lemma 6, the triggered threshold satisfies $\eta_i(t)/\theta + c_0 + c_1 e^{-\rho t} \leqslant s_i/\theta + c_0 + c_1 e^{-\rho T}$ for all $t > T$ and $i \in \mathcal{N}$. Based on Theorem 1,

selecting small values for $c_0 > 0$ and $c_1 > 0$, and large values for $\theta > 0$ and $T > 0$ can ensure that $\|\delta_{wi}(t)\|$ remains small.

Remark 6. The design of the event-triggered parameters $\theta \geqslant 0$, $c_0 > 0$, $c_1 \geqslant 0$, and $\rho > 0$ inherently involves a trade-off between communication load, quantified by the number of triggering events, and identification accuracy, measured by the mean approximation error during the steady-state phase. The parameters c_0, c_1, and ρ define a static event-triggered threshold [37,38], characterized by an exponentially decaying boundary of the form $c_0+c_1\mathrm{e}^{-\rho t}$. This threshold is predetermined and remains fixed throughout data exchange, without adaptive adjustment. During the transient phase of DCL, all agents have not yet sufficiently learned their unknown dynamics, rendering inter-agent communication both inefficient and unreliable. The funnel-shaped static threshold thus serves to suppress unnecessary triggering events in this transient regime. Notably, increasing c_0 or c_1, or decreasing ρ, generally reduces triggering frequency but may amplify the NN weight triggering error $\|\delta_{wi}(t)\|$, thereby compromising cooperative identification accuracy. In contrast, the proposed dynamic event-triggered boundary is expressed as $\eta_i(t)/\theta + c_0 + c_1\mathrm{e}^{-\rho t}$, where the internal dynamic variable $\eta_i(t)$ adapts online according to the NN weight triggering error $\|\delta_{wi}(t)\|$. The parameter θ scales the contribution of $\eta_i(t)$ to the overall triggering threshold. In the limiting case $\theta \to +\infty$, the dynamic boundary reduces to the static one, recovering the conventional design. While a moderate reduction in θ can further decrease triggering frequency and alleviate communication burden, an excessively small θ may lead to an increase in the state estimate error $\|\tilde{x}\|$ (see (29)) and consequently degrade the identification accuracy, as implied by the perturbation term in (36).

Remark 7. Although communication load among agents is reduced for the proposed dynamic event-triggered laws (16)–(18), an internal computational burden is introduced locally owing to the introduction of internal variables $\eta_i,\ i \in \mathcal{N}$. This reflects a classical "computation for communication" trade-off, where communication resources are typically more constrained than computational resources in multi-agent systems. The mechanism introduces a one-dimensional internal variable per agent, enhancing adaptability by maintaining communication during transients and reducing transmissions in steady states. The added computational cost is minimal, whereas communication savings are substantial, particularly when NN weight dimensions are large. Hence, for long-term distributed cooperative identification under limited communication resources, the dynamic event-triggered strategy achieves an effective balance, significantly lowering communication demands with only modest computational overhead.

5 Simulation results

In this section, the effectiveness and advantages of the proposed distributed DCL algorithm are demonstrated through a simulation experiment. Consider the following unknown nonlinear multi-agent system [38]:

$$\begin{cases} \dot{x}_{i1} = x_{i1}x_{i2}\exp\left(-x_{i1}^2 - x_{i2}^2\right) - \left(x_{i1} - u_i(t)\right), \\ \dot{x}_{i2} = \dfrac{x_{i1} + x_{i2}}{x_{i1}^2 + x_{i2}^2} - \left(x_{i2} - u_i(t)\right), \quad i = 1, 2, 3, 4, \end{cases} \tag{48}$$

where the system inputs $u_i(t)$ are, respectively, generated by the following four Mackey-Glass time-delay chaotic systems:

$$\begin{aligned} \dot{u}_1 &= \frac{10\left(u_1(t-8) + 0.9\right)}{1 + \left(\left(u_1(t-8) + 0.9\right)/0.8\right)^{10}} - 2\left(u_1 + 0.9\right), \\ \dot{u}_2 &= \frac{10\left(u_2(t-8.2) + 0.4\right)}{1 + \left(\left(u_2(t-8.2) + 0.4\right)/0.7\right)^{10}} - 2\left(u_2 + 0.4\right), \\ \dot{u}_3 &= \frac{10\left(u_3(t-8.5) + 1\right)}{1 + \left(\left(u_3(t-8.5) + 1\right)/0.6\right)^{10}} - 2\left(u_3 + 1\right), \\ \dot{u}_4 &= \frac{10\left(u_4(t-10) - 2\right)}{1 + \left(\left(u_4(t-10) - 2\right)/0.5\right)^{10}} - 2\left(u_4 - 2\right) \end{aligned} \tag{49}$$

with initial conditions $[u_1(t), u_2(t), u_3(t), u_4(t)] = [-0.1, 1, 1.4, 1.8]$ $(t < 0)$, and $[u_1(0), u_2(0), u_3(0), u_4(0)] = [-0.1, -1.4, 1.4, 1.8]$. The Mackey-Glass chaotic system is adopted to generate the input signals for the multi-agent network. This choice is motivated by the system's well-known nonlinear and chaotic properties, as well as its standard use as a benchmark for evaluating identification and prediction algorithms [38]. Its complex dynamics effectively test the cooperative learning capability, nonlinear approximation, and communication efficiency of the proposed DCL framework. For the multi-agent system (48), our objective is to identify the following unknown nonlinear system

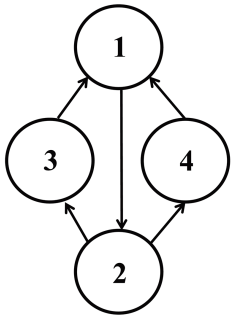

Figure 2 Communication topology.

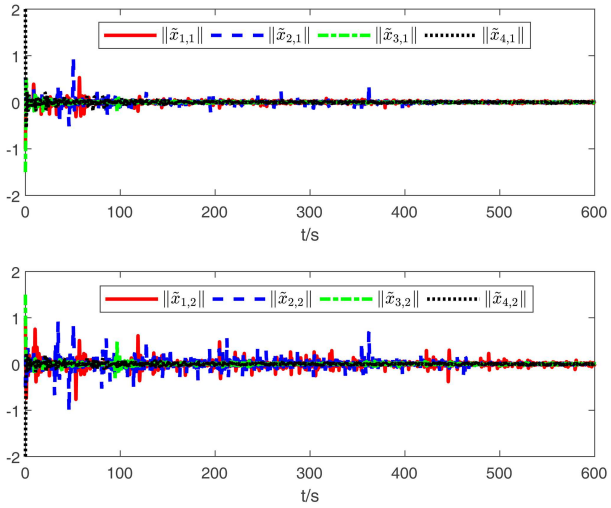

Figure 3 (Color online) State estimate errors.

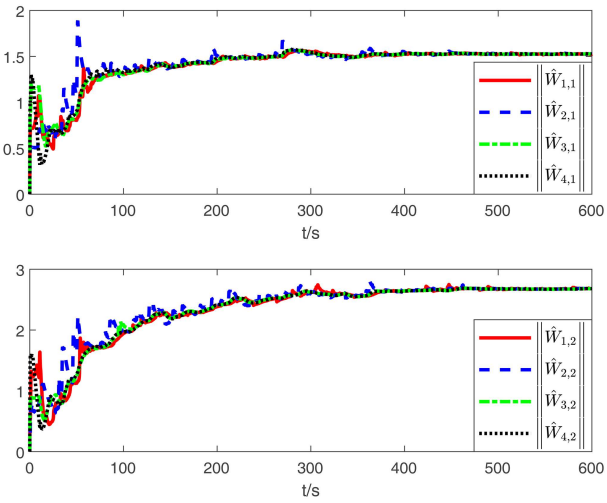

Figure 4 (Color online) The norms of NN weight estimates.

functions

$$H\left(x_i,u_i\right)=\left[h_1\left(x_i,u_i\right),h_2\left(x_i,u_i\right)\right]^{\top}=\begin{bmatrix}x_{i1}x_{i2}\exp\left(-x_{i1}^2-x_{i2}^2\right)-\left(x_{i1}-u_i\right)\\ \dfrac{x_{i1}+x_{i2}}{x_{i1}^2+x_{i2}^2}-\left(x_{i2}-u_i\right)\end{bmatrix}. \tag{50}$$

The Gaussian RBF NNs $W_j^{\top}\Phi_j(\xi_i)$ $(j=1,2)$ are constructed using 9621 neural nodes, which are uniformly distributed in a lattice $[-3,3]\times[-3,3]\times[-3,3]$ with a width of 0.5. The design parameters are selected as follows: $k_{i1}=k_{i2}=0.5$, $\Gamma_i=I$, $\sigma_i=0.00001$, $\tau_i=0.1$, $c_0=0.001$, $c_1=5$, $\theta=0.1$, and $\rho=0.1$. The initial conditions are set as $x_1(0)=[1,-1]^{\top}$, $x_2(0)=[-0.5,0.5]^{\top}$, $x_3(0)=[1.5,-1.5]^{\top}$, $x_4(0)=[-2,2]^{\top}$, $\hat{x}_i=[0,0]^{\top}$, and $\eta_i(0)=1$, $i=1,2,3,4$. The information interaction topology among the four agents is illustrated in Figure 2. It is evident that the communication topology depicted in Figure 2 is a directed connected graph, which differs from those presented in previous studies [29–31, 34–38].

After conducting the simulation based on the proposed DCL algorithm, we obtain the simulation results shown in Figures 3–7. The entire simulation duration and sampling time are set to 600 and 0.1 s, respectively. Figure 3 illustrates the state estimate errors of the established identifiers for all agents. From Figure 3, it is clear that all state estimate errors remain bounded and converge to a small neighborhood around zero. It can be seen from Figure 4 that the NN weight estimates norms of four agents converge uniformly to a unique value. Figure 5 depicts the time variations of internal dynamic variables, and it is clear from Figure 5 that the internal dynamic variables $\eta_i(t)$ $(i=1,2,3,4)$ generated by (17) remain nonnegative and ultimately converge to the origin, consistent with Lemma 6. During the steady-state process, we can obtain the constant weights $\bar{W}_{i,j}=\text{mean}_{t\in[580,600]}\hat{W}_{i,j}(t)$ $(i=1,2,3,4;\ j=1,2)$. According to Figure 7, the NN approximators with constant weights $\bar{W}_{1,j}^{\top}\Phi_j(\xi_i)$ $(i=1,2,3,4;\ j=1,2)$ achieve excellent fitting performance for the nonlinear functions $h_j(\xi_i)$. Moreover, when the constant weights $\bar{W}_{1,j}$ $(j=1,2)$ are replaced by $\bar{W}_{i,j}$ $(j=1,2)$ with $i=2,3,4$, the approximation performance for the nonlinear functions $h_j(\xi_i)$ remains excellent. This indicates that the NN weight estimates from one agent are applicable in a close region around the union trajectory, rather than just a single trajectory of a specific agent.

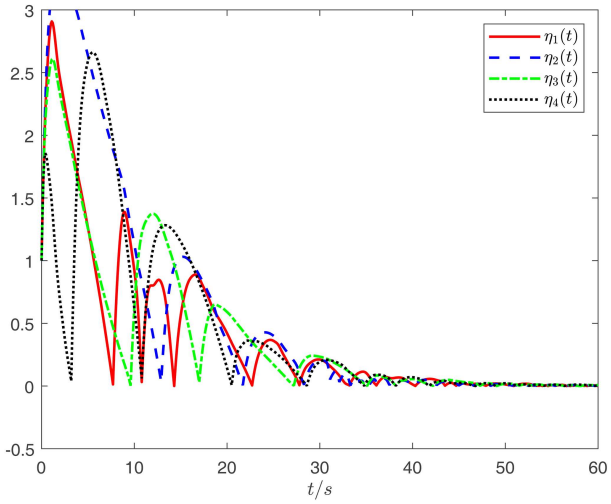

Figure 5 (Color online) Evolutions of internal dynamic variables $\eta_i(t)$, $i = 1, 2, 3, 4$.

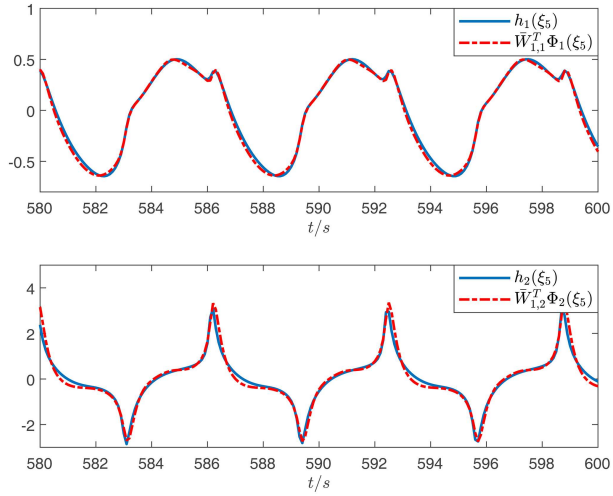

Figure 6 (Color online) Approximation performance under the input $u_5 = 0.8\sin(t)$.

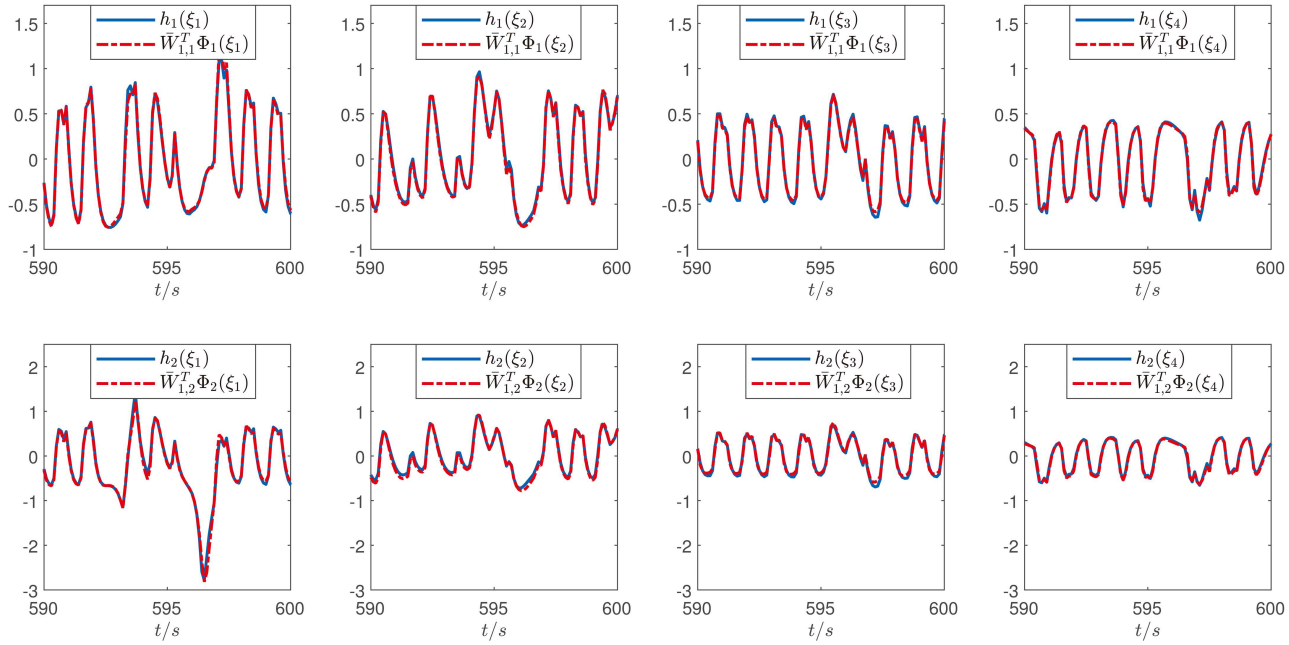

Figure 7 (Color online) Function approximation performance of four agents.

To demonstrate the advantages of the proposed dynamic event-triggered mechanism, comparisons with the following three distinct communication models are presented as follows.

(1) Time-triggered communication (TTC). In this scenario, each agent transmits its weights to its neighbors at the sampling time.

(2) Event-triggered communication with an exponentially decaying threshold (ETCWEDT) [37, 38]. The event-triggered threshold is set as $c_0 + c_1 e^{-\rho t}$.

(3) Event-triggered communication with a dynamically varying threshold (ETCWDVT). The event-triggered threshold is set as $c_0 + c_1 e^{-\rho t} + \eta_i(t)/\theta$, as applied in this work.

Figure 8 demonstrates the time variation of the weight triggering error norms using our proposed ETCWEDT mechanism. From Figure 8, it can be seen that at certain times, the weight triggering error norms exceed the threshold $c_0 + c_1 e^{-\rho t}$ but remain below $c_0 + c_1 e^{-\rho t} + \eta_i(t)/\theta$. This indicates that the introduction of internal dynamic variables $\eta_i(t)$ can effectively increase the triggering thresholds. Table 1 displays the mean triggered times and mean approximation errors when applying RBF NNs for the four agents under different communication

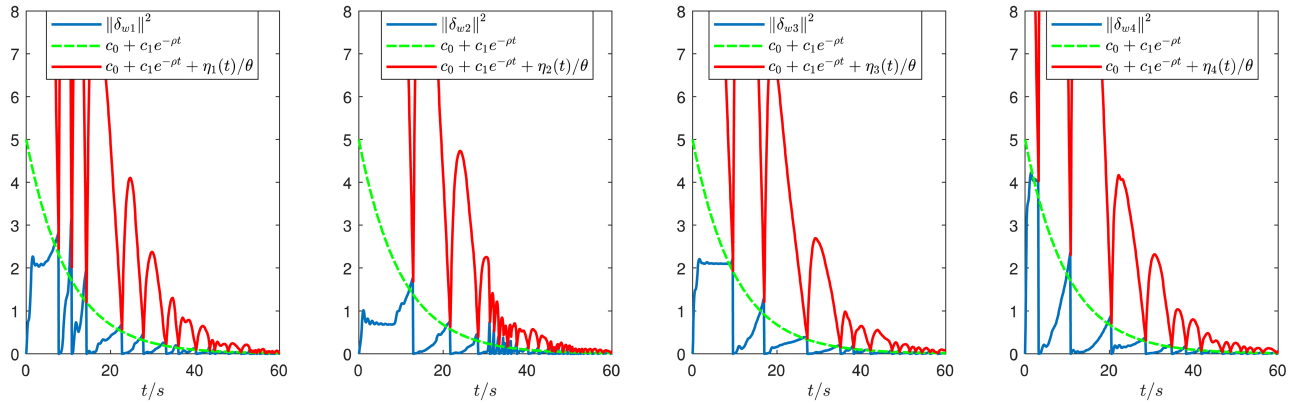

Figure 8 (Color online) Two norms of weight triggering errors and different thresholds.

Table 1 Triggering numbers under three communication models. $\mathrm{MAE}_{[550,600]}$ denotes the mean approximation error of four agents over $[550, 600]$, i.e., $1/4\sum_{i=1}^{4}\int_{t=550}^{600}|h_j(\xi_i(t))-\bar{W}_{1,j}^{\top}\Phi_j(\xi_i(t))|dt$.

Communication models	Mean triggered times	Triggered rate (%)	$\mathrm{MAE}_{[550,600]}$ for h_j $(j=1,2)$
TTC	6000	100	0.020/0.031
ETCWEDT	1285	21.42	0.021/0.034
ETCWDVT	693	11.55	0.019/0.036

models. Compared to TTC and ETCWEDT, our proposed ETCWDVT mechanism significantly reduces the number of event-triggered times while maintaining good approximation performance.

Furthermore, we conducted another simulation with a new input $u_5 = 0.8\sin(t)$, which is significantly different from the previous inputs. The approximation performance for the nonlinear function $h_j(\xi_5)$ $(j = 1, 2)$ using the learned constant weights $\bar{W}_{1,1}$ and $\bar{W}_{1,2}$ is shown in Figure 6. As shown in Figure 6, the approximation performance of the NNs remains excellent, indicating that the fitting domain of the learned NNs is well generalized.

6 Conclusion

This paper presented a distributed cooperative learning identification algorithm incorporating a dynamic event-triggered mechanism over directed connected graphs for uncertain multi-agent systems. RBF NNs were utilized to approximate the unknown system dynamics, and all agents exchanged their weight estimates via the dynamic event-triggered communication. To address the challenges arising from the non-symmetric nature of Laplacian matrices associated with directed connected graphs, a parametric Lyapunov function was employed to perform stability analysis of the entire identification error system. Furthermore, a novel group-convergence-proof strategy was proposed to ensure that the NN weight estimates converge to a small neighborhood of their common optimal values by employing Lyapunov functions, the converse Lyapunov lemma, and the directed trees lemma. Additionally, internal dynamic variables were introduced to adaptively adjust the triggering thresholds, thereby effectively extending the thresholds and reducing the number of triggering events. The learning accuracy was guaranteed while using less communication data. The learned knowledge with weight sharing among agents was applicable in the domain around the union trajectory of all agents. Future research directions in cooperative DL may focus on three key aspects: cooperative learning under more lenient excitation conditions [51, 52], the development of disturbance-observer-enhanced learning algorithms, and experimental validation in practical implementations.

Acknowledgements This work was supported by National Natural Science Foundation of China (Grant Nos. 62473162, 42227901, 62273156, U24A20329), Guangdong Basic and Applied Basic Research Foundation (Grant Nos. 2024B1515120024, 2024B1515120013), and Guangdong Emergency Management Science and Technology Program (Grant No. 2025YJKJ002).

References

1 Chen T, Zeng C, Wang C. Fault identification for a class of nonlinear systems of canonical form via deterministic learning. IEEE Trans Cybern, 2022, 52: 10957–10968
2 Chen T, Wang C, Hill D J. Rapid oscillation fault detection and isolation for distributed systems via deterministic learning. IEEE Trans Neural Netw Learn Syst, 2014, 25: 1187–1199
3 Yu C, Wang Q G, Zhang D, et al. System identification in presence of outliers. IEEE Trans Cybern, 2016, 46: 1202–1216
4 Yao X Q, Xu X M, He W, et al. Asymptotical event-based input-output constrained boundary control of flexible manipulator agents under a signed digraph. Sci China Inf Sci, 2025, 68: 142201

5 Liu Y, Yao X, Zhao W. Distributed neural-based fault-tolerant control of multiple flexible manipulators with input saturations. Automatica, 2023, 156: 111202
6 Meindl M, Bachhuber S, Seel T. Iterative model learning and dual iterative learning control: a unified framework for data-driven iterative learning control. IEEE Trans Automat Control, 2025, 70: 7818–7829
7 Liu W, Luo J, Sun W. Robust output regulation with prescribed performance for second-order non-polynomial nonlinear systems. IEEE Trans Automat Sci Eng, 2025, 22: 14234–14246
8 Sanner R M, Slotine J J E. Gaussian networks for direct adaptive control. IEEE Trans Neural Netw, 1992, 3: 837–863
9 Zhang Y, Chai T, Wang D. An alternating identification algorithm for a class of nonlinear dynamical systems. IEEE Trans Neural Netw Learn Syst, 2017, 28: 1606–1617
10 Guo K, Zheng D D, Li J. Optimal bounded ellipsoid identification with deterministic and bounded learning gains: design and application to Euler-Lagrange systems. IEEE Trans Cybern, 2022, 52: 10800–10813
11 Li H, Bai L, Wang L, et al. Adaptive neural control of uncertain nonstrict-feedback stochastic nonlinear systems with output constraint and unknown dead zone. IEEE Trans Syst Man Cybern Syst, 2017, 47: 2048–2059
12 Yao X, Li X, Liu Z, et al. Asymptotical fault-tolerant time-varying tracking control of networked mobile flexible manipulators under prescribed performances and DoS attacks. IEEE Trans Automat Control, 2026, 71: 20–35
13 Cui R, Yang C, Li Y, et al. Adaptive neural network control of AUVs with control input nonlinearities using reinforcement learning. IEEE Trans Syst Man Cybern Syst, 2017, 47: 1019–1029
14 Liu Y, Chen X B, Mei Y F, et al. Observer-based boundary control for an asymmetric output-constrained flexible robotic manipulator. Sci China Inf Sci, 2022, 65: 139203
15 Xu B, Yuan Y. Two performance enhanced control of flexible-link manipulator with system uncertainty and disturbances. Sci China Inf Sci, 2017, 60: 050202
16 Wang C, Hill D J. Learning from neural control. IEEE Trans Neural Netw, 2006, 17: 130–146
17 Liu T, Wang C, Hill D J. Learning from neural control of nonlinear systems in normal form. Syst Control Lett, 2009, 58: 633–638
18 Dai S L, Wang C, Wang M. Dynamic learning from adaptive neural network control of a class of nonaffine nonlinear systems. IEEE Trans Neural Netw Learn Syst, 2014, 25: 111–123
19 Wang M, Wang C. Learning from adaptive neural dynamic surface control of strict-feedback systems. IEEE Trans Neural Netw Learn Syst, 2015, 26: 1247–1259
20 Zhang J, Yuan C, Wu F, et al. Deterministic learning-based tracking control for parabolic PDE systems with infinite-dimensional nonlinear uncertain dynamics. IEEE Trans Automat Contr, 2025, 70: 3272–3287
21 Wang M, Zou Y, Yang C. System transformation-based neural control for full-state-constrained pure-feedback systems via disturbance observer. IEEE Trans Cybern, 2022, 52: 1479–1489
22 Shi H, Wang M, Wang C. Leader-follower formation learning control of discrete-time nonlinear multiagent systems. IEEE Trans Cybern, 2023, 53: 1184–1194
23 Wang M, Wen P, Xie X, et al. A new neural dynamic learning framework for discrete-time strict-feedback systems: internal interaction-based weight adaptive laws. IEEE Trans Cybern, 2024, 54: 4216–4228
24 Li D, Han H, Qiao J. Deterministic learning-based adaptive neural control for nonlinear full-state constrained systems. IEEE Trans Neural Netw Learn Syst, 2023, 34: 5002–5011
25 Wu W, Hu J, Zhang F, et al. New results on rapid dynamical pattern recognition via deterministic learning from sampling sequences. IEEE Trans Neural Netw Learn Syst, 2024, 35: 12330–12343
26 Wang M, Shi H T, Wang C, et al. Neural learning control for discrete-time nonlinear systems in pure-feedback form. Sci China Inf Sci, 2022, 65: 122206
27 Zeng Y, Zhang F K, Chen T R, et al. Deterministic learning-based neural output-feedback control for a class of nonlinear sampled-data systems. Sci China Inf Sci, 2024, 67: 192202
28 Luo J, Liu W. Leader-following consensus with prescribed performance for linear multiagent systems. IEEE Trans Automat Contr, 2025, 70: 1402–1409
29 Chen W, Wen C, Hua S, et al. Distributed cooperative adaptive identification and control for a group of continuous-time systems with a cooperative PE condition via consensus. IEEE Trans Automat Contr, 2014, 59: 91–106
30 Chen W, Hua S, Zhang H. Consensus-based distributed cooperative learning from closed-loop neural control systems. IEEE Trans Neural Netw Learn Syst, 2015, 26: 331–345
31 Chen W, Hua S, Sam Ge S. Consensus-based distributed cooperative learning control for a group of discrete-time nonlinear multi-agent systems using neural networks. Automatica, 2014, 50: 2254–2268
32 Abdelatti M, Yuan C Z, Zeng W, et al. Cooperative deterministic learning control for a group of homogeneous nonlinear uncertain robot manipulators. Sci China Inf Sci, 2018, 61: 112201
33 Yuan C, He H, Wang C. Cooperative deterministic learning-based formation control for a group of nonlinear uncertain mechanical systems. IEEE Trans Ind Inf, 2019, 15: 319–333
34 Dai S L, He S, Ma Y, et al. Distributed cooperative learning control of uncertain multiagent systems with prescribed performance and preserved connectivity. IEEE Trans Neural Netw Learn Syst, 2021, 32: 3217–3229
35 Dai S L, He S, Ma Y, et al. Cooperative learning-based formation control of autonomous marine surface vessels with prescribed performance. IEEE Trans Syst Man Cybern Syst, 2022, 52: 2565–2577
36 Song Z, Wu Z, Huang H. Cooperative learning formation control of multiple autonomous underwater vehicles with prescribed performance based on position estimation. Ocean Eng, 2023, 280: 114635
37 Gao F, Chen W, Li Z, et al. Neural network-based distributed cooperative learning control for multiagent systems via event-triggered communication. IEEE Trans Neural Netw Learn Syst, 2020, 31: 407–419
38 Gao F, Chen W, Li Z, et al. Neural network-based cooperative identification for a class of unknown nonlinear systems via event-triggered communication. IEEE Trans Syst Man Cybern Syst, 2021, 51: 1404–1413
39 Yu W, Chen G, Cao M. Consensus in directed networks of agents with nonlinear dynamics. IEEE Trans Automat Contr, 2011, 56: 1436–1441

40 Ren W, Beard R W. Consensus seeking in multiagent systems under dynamically changing interaction topologies. IEEE Trans Automat Contr, 2005, 50: 655–661

41 Ni J, Shi P, Zhao Y, et al. Fixed-time output consensus tracking for high-order multi-agent systems with directed network topology and packet dropout. IEEE CAA J Autom Sin, 2021, 8: 817–836

42 Wu B, Liu W. Event-triggered cooperative exponential practical tracking for a class of higher-order uncertain nonlinear multiagent systems. IEEE Trans Syst Man Cybern Syst, 2023, 53: 6931–6942

43 Girard A. Dynamic triggering mechanisms for event-triggered control. IEEE Trans Automat Contr, 2015, 60: 1992–1997

44 Shahvali M, Polycarpou M M. Event-triggered control for nonlinear uncertain strict-feedback systems: an adaptive filtering approach. IEEE Trans Automat Contr, 2025, 70: 2675–2682

45 Shahvali M, Naghibi-Sistani M B, Javad A. Distributed adaptive dynamic event-based consensus control for nonlinear uncertain multi-agent systems. J Syst Control Eng, 2022, 236: 1630–1648

46 Khalil H K. Nonlinear System. Upper Saddle River: Prentice, 2002

47 Zhang H, Lewis F L. Adaptive cooperative tracking control of higher-order nonlinear systems with unknown dynamics. Automatica, 2012, 48: 1432–1439

48 Loría A, Panteley E. Uniform exponential stability of linear time-varying systems: revisited. Syst Control Lett, 2002, 47: 13–24

49 Wang S, Zhang H, Chen Z. Adaptive cooperative tracking and parameter estimation of an uncertain leader over general directed graphs. IEEE Trans Automat Control, 2023, 68: 3888–3901

50 Fisher M E, Fuller A T. On the stabilization of matrices and the convergence of linear iterative processes. Math Proc Camb Phil Soc, 1958, 54: 417–425

51 Tan L N, Tran H T, Tran T T. Event-triggered observers and distributed H^{∞} control of physically interconnected nonholonomic mechanical agents in harsh conditions. IEEE Trans Syst Man Cybern Syst, 2022, 52: 7871–7884

52 Kamalapurkar R, Reish B, Chowdhary G, et al. Concurrent learning for parameter estimation using dynamic state-derivative estimators. IEEE Trans Automat Contr, 2017, 62: 3594–3601